Received: 28 September 2017 | Revised: 2 March 2018 | Accepted: 3 March 2018

DOI: 10.1111/mec.14567

ORIGINAL ARTICLE

WILEY MOLECULAR ECOLOGY

Pliocene–Pleistocene ecological niche evolution shapes the phylogeography of a Mediterranean plant group

C. Benítez-Benítez[1] | M. Escudero[2] | F. Rodríguez-Sánchez[3] | S. Martín-Bravo[1,†] | P. Jiménez-Mejías[4,†]

[1]Área de Botánica, Departamento de Biología Molecular e Ingeniería Bioquímica, Universidad Pablo de Olavide, Seville, Spain

[2]Department of Plant Biology and Ecology, University of Seville, Seville, Spain

[3]Departamento de Ecología Integrativa, Estación Biológica de Doñana, Consejo Superior de Investigaciones Científicas, Seville, Spain

[4]Department of Botany, Smithsonian Institution, Washington, DC, USA

Correspondence
C. Benítez-Benítez, Área de Botánica, Departamento de Biología Molecular e Ingeniería Bioquímica, Universidad Pablo de Olavide, Seville, Spain.
Email: cbenben1@upo.es

Funding information
Spanish Ministry of Economy and Competitiveness, Grant/Award Number: CGL2016-77401-P

Abstract

Estimating species ability to adapt to environmental changes is crucial to understand their past and future response to climate change. The Mediterranean Basin has experienced remarkable climatic changes since the Miocene, which have greatly influenced the evolution of the Mediterranean flora. Here, we examine the evolutionary history and biogeographic patterns of two sedge sister species (*Carex*, Cyperaceae) restricted to the western Mediterranean Basin, but with Pliocene fossil record in central Europe. In particular, we estimated the evolution of climatic niches through time and its influence in lineage differentiation. We carried out a dated phylogenetic–phylogeographic study based on seven DNA regions (nDNA and ptDNA) and fingerprinting data (AFLPs), and modelled ecological niches and species distributions for the Pliocene, Pleistocene and present. Phylogenetic and divergence time analyses revealed that both species form a monophyletic lineage originated in the late Pliocene–early Pleistocene. We detected clear genetic differentiation between both species with distinct genetic clusters in disjunct areas, indicating the predominant role of geographic barriers limiting gene flow. We found a remarkable shift in the climatic requirements between Pliocene and extant populations, although the niche seems to have been relatively conserved since the Pleistocene split of both species. This study highlights how an integrative approach combining different data sources and analyses, including fossils, allows solid and robust inferences about the evolutionary history of a plant group since the Pliocene.

KEYWORDS
allopatric speciation, *Carex* sect. *Phacocystis*, genetic structure, niche conservatism, niche differentiation, species distribution modelling

1 | INTRODUCTION

The interplay of ecological and evolutionary processes shapes the distribution of species and the dynamics of speciation, dispersal, adaptation and extinction, which results from geological and climatic changes (Lavergne, Mouquet, Thuiller, & Ronce, 2010; Webb, Ackerly, McPeek, & Donoghue, 2002). Therefore, to explain biogeographic and speciation patterns, it is crucial to understand how ecological requirements evolve through time. An increasing number of studies on the evolution of species climatic niches show that, although negligible niche change may happen since the split of sister lineages (phylogenetic niche conservatism, PNC; Ackerly, 2003; Harvey & Pagel, 1991; Wiens & Graham, 2005), there are also examples of ecological innovation (niche shift) since the species' divergence (Ackerly, 2003).

One of the most recognized signatures of niche conservatism is the similarity of ecological preferences among closely related species

[†]Both authors contributed equally to the senior authorship.

(Losos, 2008; Wiens & Graham, 2005), hypothesis previously identified by Darwin (1859) as a consequence of their relatively recent common ancestry. In addition to shared ancestry, Grafen (1989) proposed that niche similarity is also due to shared environmental constraints and biogeographic history (Crisp & Cook, 2012; Losos, 2008; Wiens & Graham, 2005). The niche conservatism idea has played an important role particularly in relation to climate change impacts (Thuiller, 2003), as climatic tolerance limits the ranges of species (Wiens & Graham, 2005), even at very large geographical and evolutionary scales (Crisp et al., 2009; Mairal, Sanmartín, & Pellissier, 2017). Holt (1996) related the absence of evolutionary change with the difficulty for adaptive traits to evolve and stabilize in novel ecological conditions. However, niches are rarely considered completely conserved due to processes of local adaptation (Thompson, 2005; Wiens & Graham, 2005). In particular, the presence of barriers that limit expansion (e.g., mountain ranges; Taberlet, Fumagalli, Wust-Saucy, & Cosson, 1998) may play a key role for niche evolution in allopatric speciation (Wiens, 2004a), as the adaptation to ecological conditions could be associated with the constraints imposed in different microhabitat preferences (Thompson, 2005). Moreover, recent studies have demonstrated that niche differences could not always be related to phylogenetic distances, as in some cases sister species have not conserved the ancestral niche (Münkemüller, Boucher, Thuiller, & Lavergne, 2015; Revell, Harmon, & Collar, 2008).

The assumption of niche conservatism has recently been further challenged based on examples of rapid niche shifts during species diversification (Evans, Smith, Flynn, & Donoghue, 2009). Only niche shift allows species to colonize and adapt to new habitats ecologically dissimilar from those on their ancestral areas (Spalink et al., 2016), or persist in the same area after an environmental change. There is also evidence of niche shifts derived from biological invasions (Broennimann et al., 2007; Stiels, Gaißer, Schidelko, Engler, & Rödder, 2015). Large-scale shifts in plant species across biomes have also been revealed (e.g., Jara-Arancio et al., 2014; Koecke, Muellner-Riehl, Pennington, Schorr, & Schnitzler, 2013). The divergence of ecologically relevant traits may have initially evolved sympatrically in the past; however, range shifts resulting in small range overlap can promote high trait divergence (Anacker & Strauss, 2014) associated with the evolutionary specialization of species to a particular climatic regime (Thompson, 2005).

The Mediterranean Basin is considered one of the Earth's hot spots of plant biodiversity regarding species richness and endemism (Médail & Quézel, 1997; Myers, Mittermeier, Mittermeier, da Fonseca, & Kent, 2000). Plant distribution patterns around the Mediterranean Basin have been of particular biogeographic interest due to the influence of complex historical geological–climatic processes and extant heterogeneous environmental conditions in this region (Médail & Diadema, 2009; Médail & Quézel, 1997; Thompson, 2005). The origin of the Mediterranean-type climate and its flora is particularly interesting from an evolutionary perspective. The Messinian Salinity Crisis (5.96–5.3 million years ago (Ma)) was a significant period of subtropical flora extinction and adaptation to aridity, triggering diversification of Mediterranean lineages (Fiz-Palacios & Valcárcel, 2013; Rodríguez-Sánchez, Pérez-Barrales, Ojeda, Vargas, & Arroyo, 2008). The progressive global cooling and local aridification already initiated during the late Miocene (Milne & Abbott, 2002; Suc et al., 1995; Thompson, 2005) culminated with the onset of the Mediterranean climatic regime during the late Pliocene (3.4–2.8 Ma). This climatic progression modified the composition and structure of the Mediterranean forests, which lost elements from the pre-existing subtropical lauroid flora and began to resemble contemporary vegetation (Thompson, 2005). Remnants of such subtropical vegetation persisted in the form of relict elements mostly at the eastern or western parts of the basin (Fernández-Mazuecos et al., 2016; Médail & Diadema, 2009; Míguez, Gehrke, Maguilla, Jiménez-Mejías, & Martín-Bravo, 2017), as well as in Mediterranean islands and Macaronesia (Médail & Diadema, 2009; Médail & Quézel, 1997). The later Quaternary climatic oscillations (starting c. 2.5 Ma), characterized by the alternation of colder (glacial) and warmer (interglacial) periods, strongly affected the distribution and genetic structure of species due to the recurrent range shifts (e.g., Gentili et al., 2015; Mansion et al., 2008). In this case, the Mediterranean Basin and Macaronesia served as glacial refugial areas (Gentili et al., 2015; Mairal et al., 2017; Médail & Diadema, 2009; Vargas, 2007), where the long-term persistence of isolated sets of populations from ancestral species frequently resulted in the formation of new allopatric lineages (Wiens, 2004b). The role of niche evolution in the biogeographic and diversification patterns of the Mediterranean Basin is crucial but still poorly understood.

Our study group is a complex of two closely related sister species, *Carex reuteriana* Boiss. and *Carex panormitana* Guss. (Cyperaceae), allopatrically distributed in the western Mediterranean Basin (Figure 1), where they inhabit creeks and river shores at low and medium altitudes (20–1,900 m; Luceño & Jiménez-Mejías, 2008). *C. reuteriana* is endemic to the Iberian Peninsula and northwestern Africa (Luceño & Jiménez-Mejías, 2008), and *C. panormitana* has a restricted distribution in Sardinia and in a few isolated populations in Sicily and Tunisia (Jiménez-Mejías, Martín-Bravo, Amini-Rad, & Luceño, 2013; Pignatti, 1982; Urbani, Gianguzzi, & Ilardi, 1995). A close phylogenetic relationship between both disjunct taxa has been recently found (Global *Carex* Group, 2016). Currently, two subspecies are accepted for *C. reuteriana* (Jiménez-Mejías, Escudero, Guerra-Cárdenas, Lye, & Luceño, 2011): (i) *C. reuteriana* ssp. *reuteriana*, which shows a patchy and disjunct distribution in the central and western Iberian Peninsula; and (ii) *C. reuteriana* ssp. *mauritanica* (Boiss. & Reut.) Jim.-Mejías & Luceño, in the southwestern Iberian Peninsula and northwestern Africa. Geographic isolation has been previously proposed as the main factor driving the diversification of *C. reuteriana* (Jiménez-Mejías et al., 2011). In contrast, the phylogeography of *C. panormitana* has not been previously studied. Interestingly, the recent study of fossil evidences has shown that the putative ancestor of *C. reuteriana*–*C. panormitana* was widely distributed throughout central Europe and western Asia during the Pliocene (Jiménez-Mejías & Martinetto, 2013; Jiménez-Mejías et al., 2016),

indicating the former presence of species of this group in areas where it is now absent.

Phylogenetic niche conservatism is the most common pattern in phylogenetic studies of species diversification (Ackerly, 2003; Crisp et al., 2009; Wiens, 2004a; Wiens et al., 2010). However, several case studies in the Mediterranean Basin suggested little niche conservatism (Donoghue, 2008; Rundel et al., 2016). We investigate the evolutionary history of the *C. reuteriana*–*C. panormitana* complex using an integrated approach comprising phylogenetic, phylogeographic and dating analyses, combined with species distribution modelling (SDM). In this study, we aimed to evaluate the amount of niche conservatism that occurred along the diversification of the *C. reuteriana*–*C. panormitana* group in the context of climate changes in the Mediterranean through the Plio–Pleistocene. In addition, we assess the phylogeographic structure to infer the main drivers of differentiation among both species and subspecies and their populations.

2 | MATERIALS AND METHODS

2.1 | Estimation of divergence times

2.1.1 | DNA amplification and matrix construction

Two nuclear (ITS and ETS-1f) and three plastid (*psb*A-*trn*H, rpl32-*trn*L^{UAG} and ycf6-psbM) regions were selected to assess the phylogenetic relationships within the Eurasian group of *Carex* sect. *Phacocystis* according to previous results by Jiménez-Mejías (2011). Fifteen samples of 12 species were obtained from silica-dried field-collected material and herbarium samples (Appendix S1). DNA extraction was performed as in Jiménez-Mejías (2011). The primers and amplification procedures for the nuclear and plastid regions followed those in Dragon and Barrington (2009), Shaw et al. (2005) and Shaw, Lickey, Schilling, and Small (2007), respectively. Sequence chromatograms were edited using GENEIOUS version 6.1.8 (Biomatters

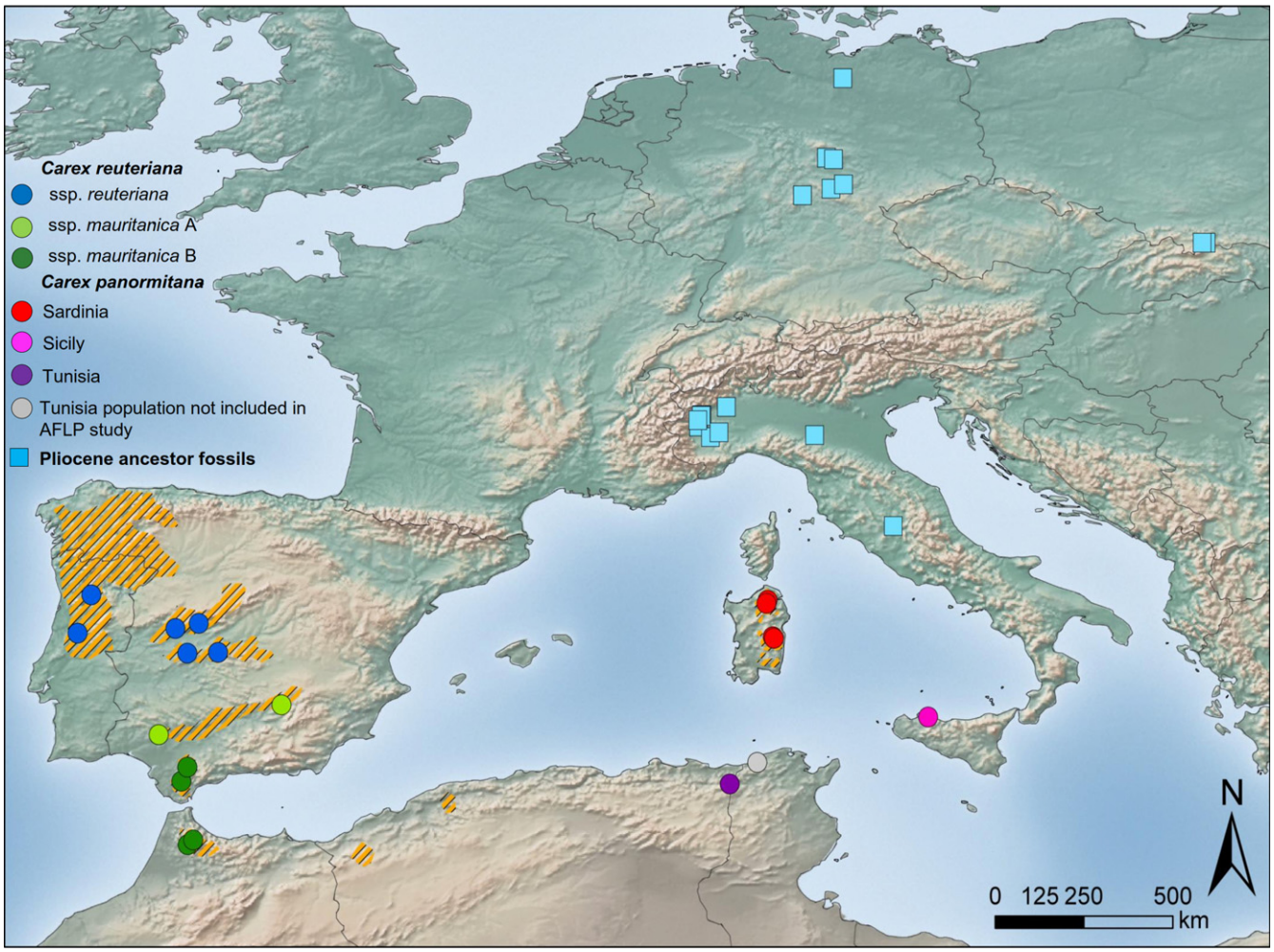

FIGURE 1 Populations used in the genetic study. Extant sampled populations are displayed with circles. *Carex reuteriana* ssp. *mauritanica* is shown in two different green tones according to the two detected subgroups (see Figure 2): (a) Sierra Morena populations and (b) South of Guadalquivir valley plus Moroccan populations. Shaded striped areas depict the approximate known distribution range of the two species according to Jiménez-Mejías et al. (2011). The unshaded populations in Sicily and Tunisia correspond to the only populations known there. Occurrences of the Pliocene fossils are displayed using squares [Colour figure can be viewed at wileyonlinelibrary.com]

Ltd., Auckland, New Zealand) and automatically aligned with MUSCLE (Edgar, 2004). Newly obtained edited sequences were included in a matrix with a representative sampling of the genus *Carex* as compiled by Míguez et al. (2017) and in Global Carex Group (2016). To this matrix, we added ITS, ETS1f, *psb*A-*trn*H and rpl32-*trn*L^{UAG} sequences from GenBank (Appendix S1). A final combined matrix consisting of 134 concatenated sequences was constructed with an aligned length of 5,211 sites. Two samples of *C. reuteriana* (one sample per *C. reuteriana* subspecies) and two samples of *Carex panormitana* (one from Sardinia and another from Sicily) were included.

2.1.2 | Dating analysis

We used a Bayesian approach to infer divergence times within *Carex* sect. *Phacocystis* and related *Carex* lineages with BEAST version 1.8.3 (Drummond & Rambaut, 2007). The availability of carefully assessed fossils is of great importance for their use as calibration points in dating analyses to obtain reliable time estimates (Tripp & McDade, 2014). Five achene fossils with an age ranging from the Late Eocene to the latest Early Pliocene (Jiménez-Mejías & Martinetto, 2013; Jiménez-Mejías et al., 2016) were applied as calibration points for the analysis (Table S1, Appendix S2). We placed all fossils on the stem nodes of the correspondent calibrated clade as their diagnostic characters could have appeared before the radiation of their respective crown groups. The only exception was *C. colwellensis*, which was placed on the deeper crown node as its associated fossil achene and utricle display synapomorphies considered currently only of *Carex* (Míguez et al., 2017). Priors for ages of fossils (see Table S1) were implemented as a lognormal distribution. We obtained the evolutionary models for each DNA region with the program JMODELTEST version 2.1.4 (Darriba, Taboada, Doallo, & Posada, 2012), and each of the five regions was treated as different subpartitions with its correspondent model: ETS and ITS under GTR + I + G model, *psb*A-*trn*H with F81, rpl32-*trn*L^{UAG} with GTR + I and ycf6-psbM under HKY model, respectively. The analysis was performed using an uncorrelated lognormal relaxed clock. We chose this clock following the comparison of its marginal likelihood against a strict clock, using Bayes factor as implemented in TRACER version 1.6 (Rambaut & Drummond, 2014), and explained in Fernández-Mazuecos, Blanco-Pastor, and Vargas (2013). Three independent MCMC runs with 150 million generations each were performed, with the parameters sampled every 10,000 generations, using a Yule speciation process as tree prior inasmuch as runs with birth–death as tree prior could not converge. Run convergence, effective sample size (ESS; values considered reliable when greater than 100) and burn-in (10%) were examined with TRACER. Trees and parameters from the three independent runs were combined using LOGCOMBINER version 1.8.3 (Drummond, Suchard, Xie, & Rambaut, 2012). A summary of the trees (maximum clade credibility, MCC tree) was calculated with TREEANNOTATOR version 1.8.3 (Drummond et al., 2012) with a posterior probability threshold above 0.5 and the mean node heights option. The resulting MCC tree was edited in FIGTREE version 1.4.0 (Rambaut, 2012).

2.2 | Population genetics

2.2.1 | Sampling

A total of 130 samples from 18 *Carex reuteriana*–*C. panormitana* populations (see Table 1; Figure 1), collected in the field and immediately stored and dried in silica gel, were used for the AFLPs (Table 1) and DNA sequence studies (Table 1). The sampling representatively covered the entire known distribution range of *C. reuteriana* (12 populations) and *C. panormitana* (six populations) with a sample size in each population ranging from three to 14 individuals. Voucher specimens were deposited in UPOS and SS herbaria. An additional Tunisian population of *C. panormitana* (Figure 1) from a herbarium voucher (M herbarium; Table 1) was included only for the DNA sequence study.

2.2.2 | AFLP study

For the AFLP procedure, we followed the protocol and selected the same primer combinations (6-FAM-*Eco*RI + AGT/*Mse*I + AGC, NED-*Eco*RI + ACC/*Mse*I + ACC and VIC-*Eco*RI + AGG/*Mse*I + CA) used by Jiménez-Mejías et al. (2011). Products were run on a capillary sequencer (ABI Prism 3700; Applied Biosystems, Foster City, CA, USA) with the internal size standard GeneScan ROX 500 (Applied Biosystems). Data collection and fragment sizing were performed using GENEMAPPER 3.7 (Applied Biosystems). Fragments in the range 50–500 bp were automatically scored and manually revised. The results were exported as a presence/absence (1/0) matrix (see Appendix S3). Reproducibility was estimated based on 12 replicated samples as the average proportion of correctly replicated bands (Bonin et al., 2004). Markers for which low reproducibility was obtained were excluded from the study.

The genetic structure of the *C. reuteriana*–*C. panormitana* complex was studied through principal coordinates analysis (PCoA) of AFLP data, with GENALEX version 6.5 as implemented in Excel (Peakall & Smouse, 2012). The complete data set and three different subpartitions were analysed separately, according to the currently accepted taxonomic entities (Jiménez-Mejías & Luceño, 2011), to explore subjacent genetic structure: (i) *C. reuteriana* s.l.; (ii) *C. reuteriana* ssp. *reuteriana*; (iii) *C. reuteriana* ssp. *mauritanica*; and (iv) *C. panormitana* s.l. We used STRUCTURE version 2.3.4 (Pritchard, Stephens, & Donnelly, 2000) to estimate the number of genetic clusters (*K*) by assigning individuals and populations in undefined mixture clusters under a Bayesian framework. We conducted 10 independent runs of 1,000,000 iterations each one, with a burn-in period of 100,000 for each value of *K* from 1 to 10. The best *K* was chosen comparing the probabilities for the *K* values inferred given the number of genetic clusters. We obtained results with both Ln Pr (X/*K*) and Δ*K* criteria (Janes et al., 2017) with STRUCTURE HARVESTER (Earl & VonHoldt, 2012). The admixture graphic was obtained with STRUCTURE PLOT (Ramasamy, Ramasamy, Bindroo, & Naik, 2014), as implemented in R (R Development Core Team, 2017).

We inferred species trees from AFLP data, with branch lengths relative to time, using a multispecies coalescent approach in SNAPP

TABLE 1 Geographic location of each sampled population of the *Carex reuteriana*– *Carex panormitana* complex, number of individuals included in each molecular study (AFLPs and DNA sequences), haplotype number (ptDNA and nDNA), indicating the number of individuals included in each one, voucher and herbarium (acronyms according to Index Herbariorum; Thiers, 2015) where specimens are deposited

Taxon/Population	Locality	Longitude/ Latitude	Ni AFLPs/Ni DNA sequences	Haplotype (ptDNA) (individuals)	Haplotype (nDNA) (individuals)	Voucher/Herbarium
C. reuteriana s.l.						
C. reuteriana ssp. *reuteriana*						
REU_POR-TM	Portugal, Tras os Montes, Lamego, Bigorne, Petrarouca	−7.88/41.03	6/5	H2(4)	H1(5)	M. Escudero et al., 37ME07 (UPOS-7374)
REU_POR-BL	Portugal, Beira Litoral, Coimbra, Lousã	−8.23/40.10	7/5	H2(5)	H1(4)/H8(1)	M. Escudero et al., 60ME07 (UPOS-7373)
REU_SPA-Av	Spain, Ávila, Sierra de Gredos, Las Chorreras del Tormes	−5.16/40.34	5/5	H2(5)	H5(2)/H6(2)/ H7(1)	J.M. Marín, 5504JMM (UPOS-1004)
REU_SPA-CcN	Spain, Cáceres, Valley of Jerte	−5.75/40.22	4/4	H2(3)	H1(3)/H7(1)	P. Jiménez-Mejías & I. Pulgar, 57PJM07 (UPOS-6957)
REU_SPA-CcS	Spain, Cáceres, Ibor river	−5.44/39.62	4/5	H2(5)	H1(3)/H3(2)	P. Jiménez-Mejías & G.E. Rodríguez, 24PJM13 (UPOS-5449)
REU_SPA-To	Spain, Toledo, Navalucillos	−4.66/39.64	3/5	H2(3)	H1(3)/H3(2)	P. Jiménez-Mejías & G.E. Rodríguez, 60PJM13 (UPOS-5479)
C. reuteriana ssp. *mauritanica*						
MAU_SPA-Se	Spain, Sevilla, El Ronquillo, Rivera de Huelva	−6.17/37.67	7/5	H3(4)	H3(5)	P. Jiménez-Mejías, 35PJM07 (UPOS-7372)
MAU_SPA-CaGu	Spain, Cádiz, El Gastor, Guadalete river	−5.45/36.88	5/5	H1(5)	H4(5)	P. Jiménez-Mejías, 34PJM07 (UPOS-7371)
MAU_SPA-CaAl	Spain, Cádiz, Alcornocales Natural Park	−5.59/36.55	8/5	H1(5)	H3(5)	P. Jiménez-Mejías & I. Pulgar, 17PJM07 (UPOS s.n.)
MAU_SPA-J	Spain, Jaén, Despeñaperros	−3.06/38.39	8/5	H3(5)	H3(5)	P. Jiménez-Mejías & L. Reina, 67PJM09 (UPOS s.n.)
MAU_MOR-Lao	Morocco, Tanger, Rif, Oued Laou	−5.30/35.14	5/5	H3(5)	H1(1)/H2(3) /H3(1)	A.J. Chaparro et al., 8AJC05 (UPOS-1637)
MAU_MOR-Lou	Morocco, Tanger, Rif, Oued Loukos	−5.44/35.03	7/5	H3(5)	H1(1)/H2(3) /H5(1)	A.J. Chaparro et al., 3AJC05 (UPOS-1630)
C. panormitana						
Tunisia–Sicily						
PAN_TUN	Tunisia, Jendouba, El Feija National Park	8.31/36.49	9/6	H3(5)	H9(6)	P. Jiménez-Mejías & G.E. Rodríguez, 132PJM13 (UPOS-6636)
PAN_TUN-Tub	Tunisia, Tubarka	9.00/37.00	—/1	H3(1)	H9(1)	J. Höller (M-0223053)
PAN_SIC	Italy, Sicily, Fiume Oreto	13.34/38.09	14/14	H3(14)	H9(10)/ H10(4)	D. Cusimano s.n. (SS)
Sardinia						
PAN_SAR-Bau	Italy, Sardinia, Bau Mela river, Villagrande	9.42/39.98	9/5	H3(5)	H9(5)	M. Urbani s.n., 2013 (SS)
PAN_SAR-Pira	Italy, Sardinia, Cantoniera, Pirae'onni, Villagrande	9.40/40.02	10/5	H3(5)	H9(5)	M. Urbani s.n., 2013 (SS)
PAN_SAR-Ber	Italy, Sardinia, Ramacaso river, Berchidda	9.24/40.82	8/5	H3(4)	H9(5)	M. Urbani s.n., 2013 (SS)
PAN_SAR-Cal	Italy, Sardinia, Miriacheddu river, Calangianus	9.26/40.89	11/5	H3(5)	H9(5)	M. Urbani s.n., 2013 (SS)

Labelling of the populations specifies the taxa (REU = *Carex reuteriana* ssp. *reuteriana*; MAU = *Carex reuteriana* ssp. *mauritanica*; PAN = *Carex panormitana*), and the country following TDWG botanical countries nomenclature (Brummitt, 2001) [MOR = Morocco, POR = Portugal, SAR = Sardinia, SIC = Sicily, SPA = Spain, TUN = Tunisia]. One of the Tunisian populations (PAN_TUN-Tub) has only been included in the DNA sequence study. Haplotype numbers are represented in the Figure S2a,b.

(Bryant, Bouckaert, Felsenstein, Rosenberg, & Roy Choudhury, 2012), a Bayesian MCMC sampler implemented in BEAST version 2.4.1 (Bouckaert et al., 2014). First, a Bayesian full coalescent model was used to estimate rate parameters and integrate over all possible gene trees. Then, a pure birth (Yule) model rate prior was implemented to estimate the species tree topology and species divergence times. We ran three Markov chain Monte Carlo (MCMC) chains with 5 million states and 10% burn-in. Trees and parameter values were sampled every 1,000 states. A combined tree was constructed sampling every 3,000 states each run. A summary of the tree (node relative age, posterior probability) was visualized with TREEANNOTATOR. Evaluation of the sampled tree from the coalescent approach to species tree reconstruction revealed an effective sample size (ESS > 200) with relative ages at each node resolved, which are directly proportional to the diversification time. The age of the tree root, corresponding to the common ancestor of the *C. reuteriana*–*C. panormitana* complex, was obtained by transforming relative to absolute divergence times using the previously crown node age of the complex previously estimated with BEAST (see above). The 95% highest posterior density (HPD) intervals were calculated both using the mean value of the crown node, and the 95% HPD interval from BEAST analysis as reference (see Table S2). The mutation rate for each lineage was estimated based on $t = T\ \mu$, where the relative (t), and absolute (T) divergence times were known. Effective population sizes were estimated based on $\theta = 4Ne\mu$ from the known θ value for each branch and the mutation rate previously calculated.

2.2.3 | Sequence study

For the plastid DNA sequence polymorphism study, we selected the most variable plastid region (rpl32-*trn*L^{UAG}), as previously detected for *C. reuteriana* in Jiménez-Mejías et al. (2011). In addition, we also amplified and tested two nuclear regions (G3PDH, CATP), which were already found to be highly variable in other *Carex* groups (Maguilla, Escudero, Waterway, Hipp, & Luceño, 2015). Primers and PCR conditions followed the two above-cited publications. Products were purified using ExoSAP (USB Corporation, Ohio, USA) and sequenced by GATC Biotech (Constance, Germany). Sequence editing was performed as explained above.

A statistical parsimony analysis was conducted with TCS version 1.2.1 (Clement, Posada, & Crandall, 2000), to calculate the most parsimonious plastid and nuclear haplotype networks with a 95% parsimony connection limit for the minimum number of mutations differentiating the obtained haplotypes. This analysis also considered extinct or not sampled haplotypes. Gaps and additivities in sequences were treated as missing data. Nuclear CATP-G3PDH regions were combined into the same matrix due to no significant incongruences found between both individual matrices after conducting a Hompart test (1,000 replicates) as implemented in PAUP* version 4.0b10 (Swofford, 2002) in a Phylocluster (California Academy of Sciences).

We estimated population parameters using a coalescent model based on the isolation-with-migration model implemented in IM$_A$2 (Hey, 2010). We followed indications according to Qiu et al. (2009), Pettengill and Moeller (2012) and Jiménez-Mejías, Fernández-Mazuecos, Amat, and Vargas (2015). We estimated divergence times, population sizes and migration rates between the four main lineages of *C. reuteriana*–*C. panormitana* complex according to AFLP results (see ALFP population genetic analyses in Section 3). The analysis explicitly accounts for the sequence divergence among lineages caused by ancestral polymorphism, so controls population size shifts at the time of divergence and postdivergence gene flow (Won & Hey, 2005). We analysed three regions as independent loci: the two nDNA (G3PDH and CATP) and the ptDNA (rpl32-*trn*L^{UAG}). The rpl32-*trn*L^{UAG} region best fitted the HKY nucleotide substitution model, and G3PDH and CATP the infinite sites model (I). A fourth locus was considered with the information from coded indels in the three DNA regions using also an infinite site model. The topology used for this analysis was obtained from the SNAPP analyses of AFLP data and the date of origin of the complex resulting from BEAST (see Multispecies coalescent AFLP analysis in Section 3). The inheritance scalar considered more appropriate was 1 for autosomal nDNA and indels and 0.5 for ptDNA to reflect the expected effective population size of an inherited locus (Pettengill & Moeller, 2012; Qiu et al., 2009). A range of mutation rates was calculated for each locus (excluding indels) based on the 95% highest posterior density interval for the crown node age of the complex. This range was estimated using DNASP version 5.1 (Librado & Rozas, 2009) to calculate the average number of nucleotide differences between populations per each locus. These ranges were included in the model to estimate parameters related to species. Population model was constrained to allow only migration between current and ancestral sister lineages. Multiple trial runs were performed in IM$_A$2 to establish an adequate set of priors in the final analyses. We performed two different runs with the selected combination of a priori maximum values for the parameters migration (m = 200), population size (q = 50) and time (t = 3) using 150 chains and five millions of generations, with a burn-in of one million generations. In each run, 5,000 trees were stored, adding up 10,000 genealogies which were used to calculate the final parameters in demographic scales using the mean mutation rates of the three DNA regions. We used a generation time of 2 years (which is the minimum for the vast majority of *Carex* species; Ball & Reznicek, 2002), as well as 5 and 10 years.

2.3 | Species distribution modelling

Information on the geographic distribution of *C. reuteriana*–*C. panormitana* and their putative fossil ancestor (*C. panormitana*-type; Table S1) was used to assess the present ecological niche and its evolution from the Pliocene to present times. The current distribution range of the complex was collected mainly from GBIF (https://www.gbif.org/) and corrected and complemented with our own field sampling (Appendix S4), bibliographic references (Gianguzzi, Cusimano, Ilardi, & Salvatore, 2013; Jiménez-Mejías, Escudero, Chaparro, & Luceño, 2007; Urbani, Calvia, & Pisanu, 2013) and herbarium specimens (COFC, SEV, and SS herbaria; Thiers, 2015). Unreliable

points due to incorrect georeferencing (e.g., populations falling in the sea or outside the known distribution range) or taxonomic issues (e.g., known misidentifications) were removed. The final data set for extant species, accurately and comprehensively representing their current distribution, was composed of 462 point localities, 433 belonging to *C. reuteriana* (315 for ssp. *reuteriana* and 118 for ssp. *mauritanica*) and 29 belonging to *C. panormitana* (which included all known populations: six close subpopulations of the only population from Sicily, two populations from Tunisia and 21 located in Sardinia). The final data set for the fossil ancestor was composed of 17 Pliocene fossil records identified as *C. panormitana*-type (Figure 1; Jiménez-Mejías et al., 2016), which were used to validate the Pliocenic palaeodistribution projection.

We retrieved 19 bioclimatic variables (resolution of 2.5 min) from WORLDCLIM (http://www.worldclim.org/; Hijmans, Cameron, Parra, Jones, & Jarvis, 2005) for current conditions and projections to the Late Quaternary; and from ECOCLIMATE (resolution of 0.5°; http://ecoclimate.org/; Lima-Ribeiro et al., 2015), for projections to the Pliocene. We also used soil pH (15 cm depth) from ISRIC (http://www.isric.org/) as environmental predictor, as *C. reuteriana* ssp. *reuteriana* is acidophilus, thus not indifferent to the substrate. We selected environmental variables based on ecological knowledge of our species and statistical criteria (Mod, Scherrer, Luoto, & Guisan, 2016). Thus, to avoid using highly correlated variables for the modelling, we calculated the absolute value of the correlation matrix converting it into a matrix of distances in the form of a dendrogram. We only selected one variable per clade when the branch was below 0.5. Furthermore, we also used the variance inflation factor (VIF), a measure of how much collinearity increases variance in a model, using HH package (Heiberger, 2017) in R (R Core Development Team, 2017). We selected variables with VIF <5, which had sound biological interpretation for our species. In the end, in addition to soil pH, we used four bioclimatic variables, two representing temperatures (bio2: mean diurnal range and bio4: temperature seasonality) and two representing precipitation (bio15: precipitation seasonality and bio16: precipitation of wettest quarter).

The maximum entropy algorithm, as implemented in MAXENT version 3.3.3 (Elith et al., 2011), was used to evaluate the potential distribution of our species complex for: (1) present times; (2) the Late Quaternary, including (2a) the last glacial maximum (LGM, c. 21ka) and (2b) the last interglacial (LIG, 120–140 ka)); and (3) the middle Pliocene (3 Ma). For model calibration, *C. reuteriana* was subdivided into two subspecies (Jiménez-Mejías et al., 2011), to account for the retrieved genetic structure (see Section 3). On the contrary, *C. panormitana* was considered as a single group. For the projection of the suitable range at the middle Pliocene, we used a model based on all extant occurrences since in that period the species most likely did not display phylogeographic structure yet, according to estimated divergence times (see Section 3). We used the same background area for all present and past projections (Figures 4 and S3). Finally, for comparison we also fitted models to the Pliocene fossil records using all 17 occurrences of *C. panormitana*-type.

For each model, we ran 100 replicates, using a random partition of 20% of the occurrences data set to test the model. We used the software default parameters, but excluding threshold and hinge features which may lead to overfitting (Merow, Smith, & Silander, 2013; Phillips, Anderson, Dudík, Schapire, & Blair, 2017). We evaluated the calibrated models by comparing response curves, area under the curve (AUC) scores and jackknife tests to select those uncorrelated variables with the highest relative contributions to the model. The retained variables were subsequently used to repeat the modelling analyses for present, Late Pleistocene and Pliocene.

In addition, the environmental niche occupied by extant taxa and Pliocene fossil records was visualized through a principal components analysis (PCA) of the retained variables using the "prcomp" function in R. We also used the function "ggbiplot" in GGPLOT2 package (Wickham, 2009) for mapping individual climatic variables into the multivariate climate space. We compared the fitted response curves for the retained variables between extant taxa and Pliocene fossils. We calculated values of Schoener's index (D) statistic for niche overlap (Schoener, 1968; Warren, Glor, & Turelly, 2008). Niche overlap between genetic groups (see Section 3) was evaluated using the niche similarity test, which assesses whether the niches of both groups are more similar than expected by chance (Warren et al., 2008). We also calculated the niche equivalency that tests whether the niches occupied by two taxa are identical (Broennimann et al., 2012; Warren et al., 2008). Schoener's D and niche similarity and equivalency tests were calculated in ECOSPAT package (Di Cola et al., 2017).

3 | RESULTS

3.1 | Estimation of divergence times from DNA sequences

Diversification of the core *Phacocystis* was estimated to have occurred during the Late Miocene (mean 7.97 Ma, 95% HPD: 4.93–10.37 Ma; Table 2a; see Figure S1). The split of the two main lineages (lineages 1 and 2, see Figure 3a) could have taken place around 6.2 Ma (95% HPD: 4.29–9.02 Ma; Figure 3a), also coinciding with Late Miocene. The stem node of *Carex panormitana–C. reuteriana* complex was dated at around 4.79 Ma (95% HPD: 3.8–6.43 Ma; Table 2a; Figure 3a) during the late Miocene–early Pliocene, while the crown node fell in the Upper–Middle Pleistocene (mean 0.95 Ma; 95% HPD: 0.19–2.48 Ma; Table 2a; Figure 3a).

3.2 | AFLP population genetic analyses

The final AFLP matrix was composed of 182 polymorphic loci for the 130 sampled individuals from 18 populations (Figure 1). The PCoA of the whole AFLP data set (Figure 2c) revealed three well-defined clusters: (i) *C. reuteriana*, comprising individuals of subspecies *reuteriana* and *mauritanica* segregated at different sides of the cluster (Figure 2d); (ii) Sardinian populations of *C. panormitana*; and (iii) Sicilian and Tunisian populations of *C. panormitana*, with a slight separation between the samples coming from each of the two areas (Figure 2e). The three first factors of the PCoA including all samples

and taxa accounted for 23.69%, 10.94% and 8.48% of the variation, respectively. The PCoA scatter plot for *C. reuteriana* ssp. *reuteriana* did not show geographical structure, whereas the PCoA performed for *C. reuteriana* ssp. *mauritanica* revealed a clear subdivision into three subclusters with geographic congruence (Jiménez-Mejías et al., 2011): (i) Iberian populations from Sierra Morena (north of Guadalquivir river valley), (ii) Iberian populations from Betic ranges (south of Guadalquivir river valley) and (iii) the northern African (Moroccan) populations. No clear geographical pattern was detected among the samples of Sardinian populations.

The STRUCTURE analysis of the whole data set using ΔK method yielded four optimal genetic clusters ($K = 4$) with taxonomic/geographic correspondence (Figure 2a). The first cluster comprised Sardinian populations of *C. panormitana*, the second one included Sicilian–Tunisian populations of *C. panormitana*, the third comprised all populations of *C. reuteriana* ssp. *mauritanica* and the last cluster incorporated the populations of the subspecies *reuteriana*. In this STRUCTURE analysis, the admixture found between groups was incidental (Figure 2a). On the other hand, the results from Ln Pr (X/*K*) tool displayed six optimal genetic clusters ($K = 6$; Figure 2b). Subspecies from *C. reuteriana* were subdivided into two clusters each one: (i) subspecies *mauritanica* into north and south of Guadalquivir valley, (ii) and subspecies *reuteriana* into one cluster constituted by two populations from CW Spain and the other one with the other populations (Figure 2b).

SNAPP analyses yielded a well-resolved topology in which both the two species (*C. reuteriana*, *C. panormitana*) and the two subspecies of *C. reuteriana* were well supported (>0.95 PP; Figure 3). The two main lineages within *C. panormitana* (Sardinia, Sicily–Tunisia) received slightly lower support (>0.85 PP; Figure 3b). The complex *C. reuteriana*–*C. panormitana* first differentiated c. 0.95 Ma at the Upper–Middle Pleistocene (95% HPD: 0.663–1.280 Ma; Figure 3b). The split between the two *C. reuteriana* subspecies took place around 0.576 Ma ago (95% HPD: 0.428–0.734 Ma; Table 2b; Figure 3b). Subspecies *mauritanica* diversified into two lineages (0.436 Ma; 95% HPD: 0.313–0.562 Ma; Table 2b; Figure 3b): (i) Iberian populations from Sierra Morena and (ii) Iberian populations from the south of Guadalquivir river valley plus the Moroccan populations. The crown node of ssp. *reuteriana* was dated back to 0.313 Ma (95% HPD: 0.205–0.436 Ma; Table 2b; Figure 3b). Divergence of the Sicilian–Tunisian lineage from the Sardinian lineage of *C. panormitana* was estimated at 0.785 Ma (86% HPD: 0.471–1.045 Ma; Table 2b; Figure 3b). The split between Sicilian and Tunisian populations was dated at 0.529 Ma ago (95% HPD: 0.313–0.755 Ma; Table 2b; Figure 3b). Finally, Sardinian populations were those that diversified most recently (0.144 Ma; 95% HPD: 0.085–0.212 Ma; Table 2b; Figure 3b). Effective population sizes from SNAPP analysis were higher for *C. reuteriana* than for *C. panormitana*; in turn, Sardinian populations belonging to the latter species were estimated to have a smaller effective size than Sicilian–Tunisian populations. However, both subspecies from *C. reuteriana* showed a similar effective population size. In addition, the common ancestor of the lineages had larger population size than subsequently divergent groups (see Table S3). As we are aware of the limitations derived from the SNAPP analysis, a detailed section about methodological concerns has been included (see Appendix S7).

TABLE 2 (a) Divergence dates of the most important clades resolved in the divergence time estimation analysis of *Carex* under an uncorrelated log-normal clock model using the combined matrix of ETS1f, ITS, *psb*A-*trn*H, rpl32-*trn*L^{UAG} and ycf6-psbM regions in BEAST (see Figures 3a and S1). Posterior probabilities, mean time to the most common recent ancestor in Ma and 95% highest posterior density (HDP) intervals are shown (see also Figure S1). (b) Divergence dates of the most important clades resolved in the divergence time estimation from AFLP data using a multispecies coalescent approach implemented in SNAPP (see Figure 3b). Posterior probabilities, mean time to the most common recent ancestor in Ma and 95% HPD intervals are shown

Clade	Posterior probability	Median (Ma)	95% HPD interval (Ma)	
			Max.	Min.
(a)				
Core *Phacocystis*	0.62	7.97	4.93	11.28
(2) Lineage A+ Lineage B	0.84	4.79	3.8	6.43
Lineage A: *Carex panormitana*–*Carex reuteriana* (Stem node)	1	0.95	0.19	2.48
Lineage B: *C. trinervis*, *C. nigra*, *C. appendiculata*, *C. cespitosa*, *C. omskiana* (Stem node)	1	3.71	3.51	4.29
(b)				
C. reuteriana	1	0.576	0.428	0.734
Iberian lineage (ssp. *reuteriana*)	1	0.313	0.205	0.436
Afro-Iberian lineage (ssp. *mauritanica*)	0.97	0.436	0.313	0.562
C. panormitana	0.86	0.785	—	—
Sardinian lineage	1	0.144	0.085	0.212
Sicilian–Tunisian lineage	0.95	0.529	0.313	0.755

3.3 | nDNA–ptDNA haplotype analyses

Statistical parsimony analysis of plastid data set revealed three haplotypes (H1-H3; Table 1; Figure S2a). The most common haplotype (H3) was shared between *C. reuteriana* ssp. *mauritanica* and *C. panormitana* (Table 1; Figure S2a). The other haplotypes were exclusive of *C. reuteriana* ssp. *reuteriana* (H2) and *C. reuteriana* ssp. *mauritanica* (H1) respectively; Table 1; Figure S2a). The nDNA network displayed ten haplotypes (H1-H10; Table 1; Figure S2b). No haplotypes were shared between *C. panormitana* and *C. reuteriana*. *Carex panormitana* displayed two haplotypes, the most common (H9) present in all sampled populations, while H10 was found in a few individuals from Sicily (Table 1; Figure S2b). *Carex reuteriana* ssp. *reuteriana* displayed six haplotypes (H1, H3 and H5-H8) and *C. reuteriana* ssp. *mauritanica*

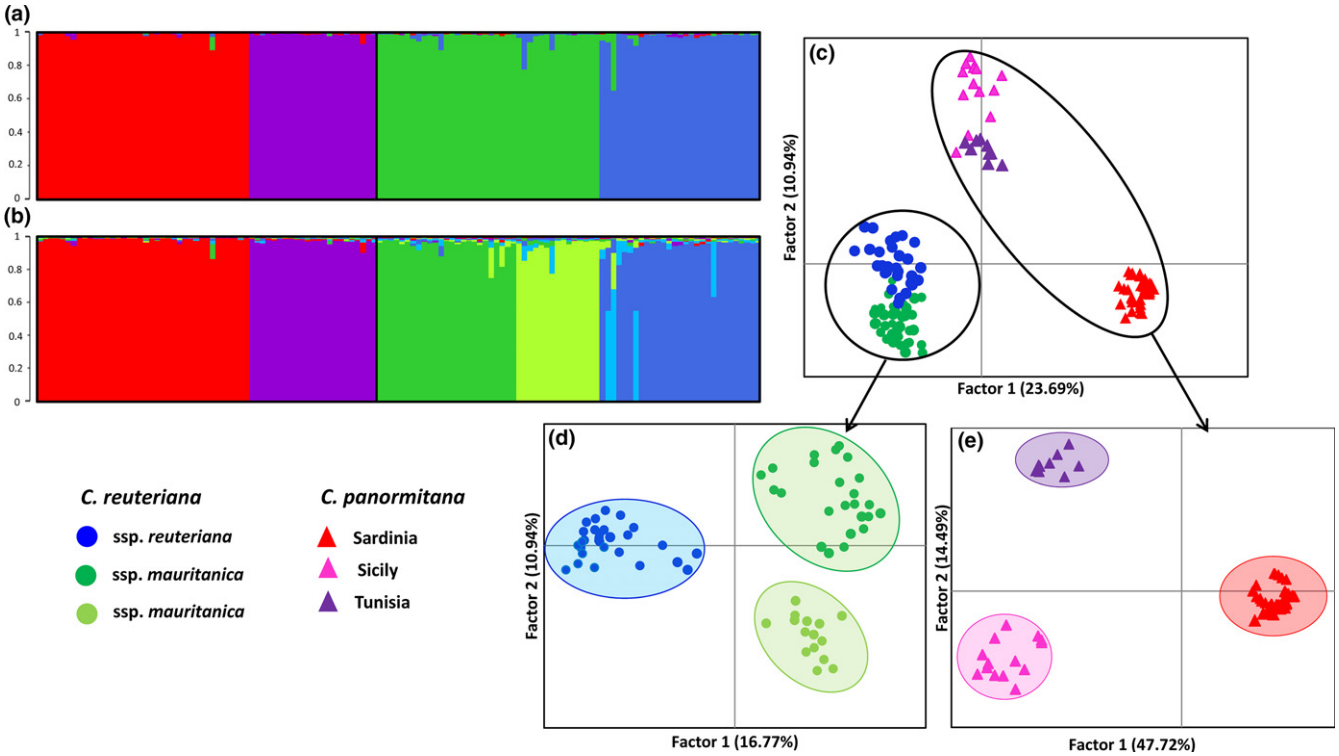

FIGURE 2 Clustering of individuals by STRUCTURE (see Section 3): each individual is represented by a vertical bar, and same colour in different individuals indicates that they belong to the same genetic cluster. The four genetic clusters ($K = 4$) retrieved in (a) correspond from left to right to: (i) Sardinian populations and (ii) Sicilian–Tunisian populations belonging to *Carex panormitana*, (iii) *Carex reuteriana* ssp. *reuteriana* and (iv) *C. reuteriana* ssp. *mauritanica*. In (b) is shown another STRUCTURE analysis result with six genetic clusters ($K = 6$) due to the subspecies *mauritanica* splitting into two subgroups (South of Guadalquivir valley plus Moroccan populations and Sierra Morena populations) and subspecies *reuteriana* splitting in other two (two CW Spain populations distinct from the rest). Principal coordinate analysis scatter plots of AFLP data from: (c) the whole data set, (d) *C. reuteriana* s.l. and (e) *C. panormitana*. Populations from *C. panormitana* are split in three different groups corresponding to each geographic area (see Figure 1) [Colour figure can be viewed at wileyonlinelibrary.com]

five haplotypes (H1-H5), the two subspecies sharing three haplotypes.

3.4 | Isolation-with-migration model

Mean divergence times estimated for the two ancestors of *C. reuteriana–C. panormitana* with the IM_A2 analysis (Figure S2c) were more recent than those obtained from the SNAPP analysis based on AFLPs (see below; Figure 3b). However, taking into account 95% confidence intervals, ages from IM_A2 (Figure S2c) were mostly congruent with those from SNAPP (Figure 3b, see Appendix S5). Additional results about estimated values of effective population size and detailed methodological caveats about IM_A2 have been included in Appendix S6 and S7, respectively.

3.5 | Species distribution modelling

The four bioclimatic variables that most contributed to the models, in addition to soil pH, were as follows: (bio2) Mean Diurnal Temperature Range (mean of monthly differences between maximum and minimum temperature), (bio4) Temperature Seasonality (standard deviation of monthly mean temperature*100), (bio15) Precipitation Seasonality (coefficient of variation of monthly precipitation), and (bio16) Precipitation of the Wettest Quarter (see Table S4). AUC values were above 0.9 for all models, which indicate good predictive ability (Swets, 1988). The potential distribution inferred by MAXENT at present for the different taxa partitions considered within the *C. reuteriana–C. panormitana* complex (Figure 4) closely matched the current populations distribution in each case (Figure 1). Projections to the LGM (21ka; Figure S3a) and LIG (120–140 ka; Figure S3b) revealed potential distributions similar to the current ones, although with a more restricted distribution for the LIG. Our two independent approaches for inferring middle Pliocene (3 Ma) distributions (i.e., projecting models calibrated with either current occurrences or Pliocene fossils) revealed similar results. In both cases, the potential distribution expanded into higher latitudes (central Europe) (Figure 4b).

Pliocene populations occupied significantly less seasonal climates (both for temperature and precipitation) than extant populations (Figure 5a). On the other hand, all three extant taxa overlapped strongly in their climatic spaces (Figure 5b): only *C. panormitana* differed in occupying climates with lower temperature oscillations and intermediate precipitation seasonality, than *C. reuteriana* subspecies (Figure 5b). The PCA revealed that Pliocene *C. panormitana*-type fossils appeared well differentiated in environmental space from

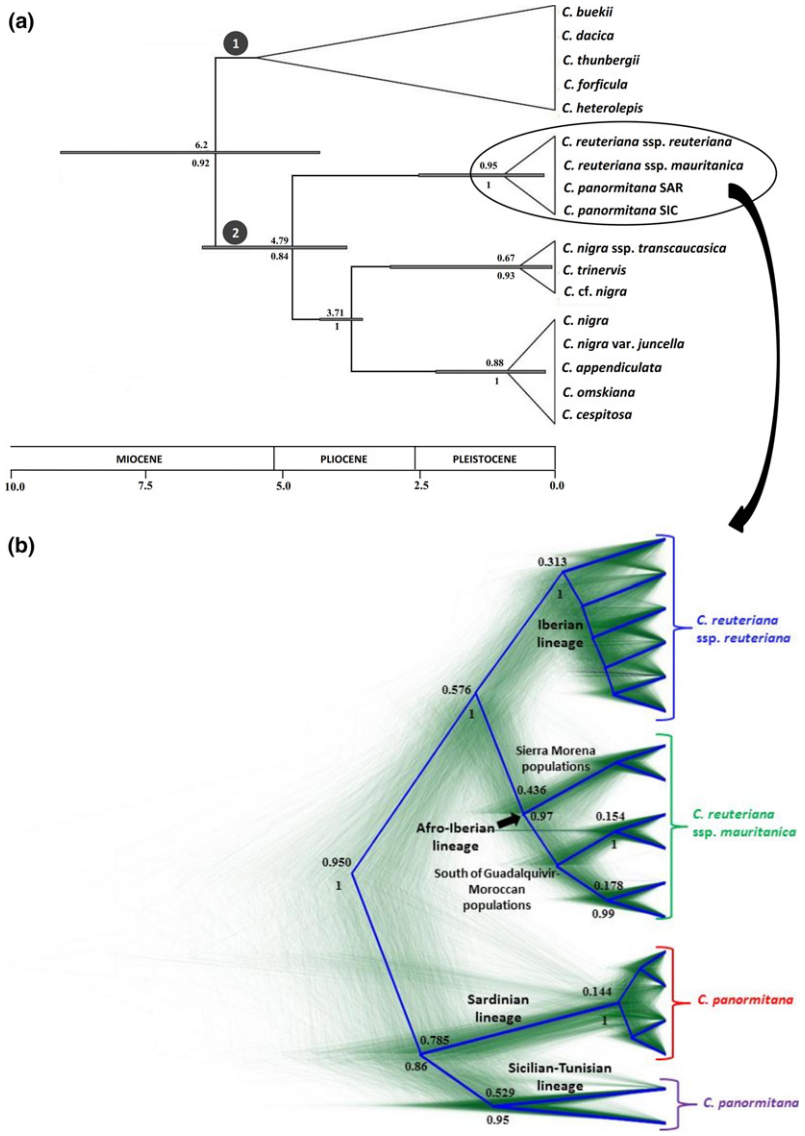

FIGURE 3 (a) Maximum-credibility-clade chronogram from the Bayesian divergence time analysis of the combined nuclear-plastid data set showing the study group and related lineages within *Carex* sect. *Phacocystis*. Branch lengths correspond to the time scale (Ma). Node ages are given above branches and posterior probability values (>0.80) below branches. Node bars represent the 95% highest posterior density (HPD) intervals for the divergence time estimates of the nodes (see Figure S1 in supporting information for the full tree). (b) Densitree of the *Carex reuteriana*–*Carex panormitana* complex showing the complete genealogical tree set (thin lines) and consensus tree (thick lines) from SNAPP analysis of AFLP data. Node ages are given above branches (Ma) and the posterior probability below branches. Both values are shown only for nodes with supports equal or greater than 0.8 [Colour figure can be viewed at wileyonlinelibrary.com]

populations of extant species (Figure 6). With respect to extant taxa, the PCA revealed an overlap between *C. reuteriana* and *C. panormitana* (Figures 5b and 6). However, all niche similarity tests failed to show niche similarity higher than expected by chance (Table 3). Pairwise statistical comparisons of ecological niches suggested that they are not significantly more similar than expected by chance (Table 3). However, values were far closer to significance (especially for the comparison between ssp. *reuteriana* and ssp. *mauritanica*) than for the comparison between fossils and extant taxa.

4 | DISCUSSION

4.1 | A vicariant genetic structure shaped by Pleistocene glaciations

We have assessed the evolutionary history, ecological niche shifts and biogeographic relationships in the *Carex reuteriana-C. panormitana* complex constituted by two sister species disjunctly distributed in the western Mediterranean. Both species form a strongly supported monophyletic group (Global Carex Group, 2016), which seems to have diverged from its closest relatives during the Pliocene (Table 2a; Figure 3a). The estimated times of diversification within this group were straitened within the Pleistocene (Table 2a; Figure 6), suggesting a role of the Pleistocene glacial–interglacial cycles, as has been inferred for other western Mediterranean plant groups (González-Martínez et al., 2010; Terrab, Schönswetter, Talavera, Vela, & Stuessy, 2008; Tremetsberger et al., 2016; among many others). The genetic structure and estimated divergence ages point to range contraction followed by isolation in different western Mediterranean glacial refugia (Iberian and Italian peninsulas, northwestern Africa, and Tyrrhenian islands; Médail & Diadema, 2009) as the most likely scenario for the speciation and population differentiation within the *C. reuteriana*–*C. panormitana* complex (Figures 2 and 3b). The harsher climatic conditions during the glacial periods seem to have resulted in the extinction of the group's ancestor from central and northwestern Europe (North Italy, Germany, Poland,

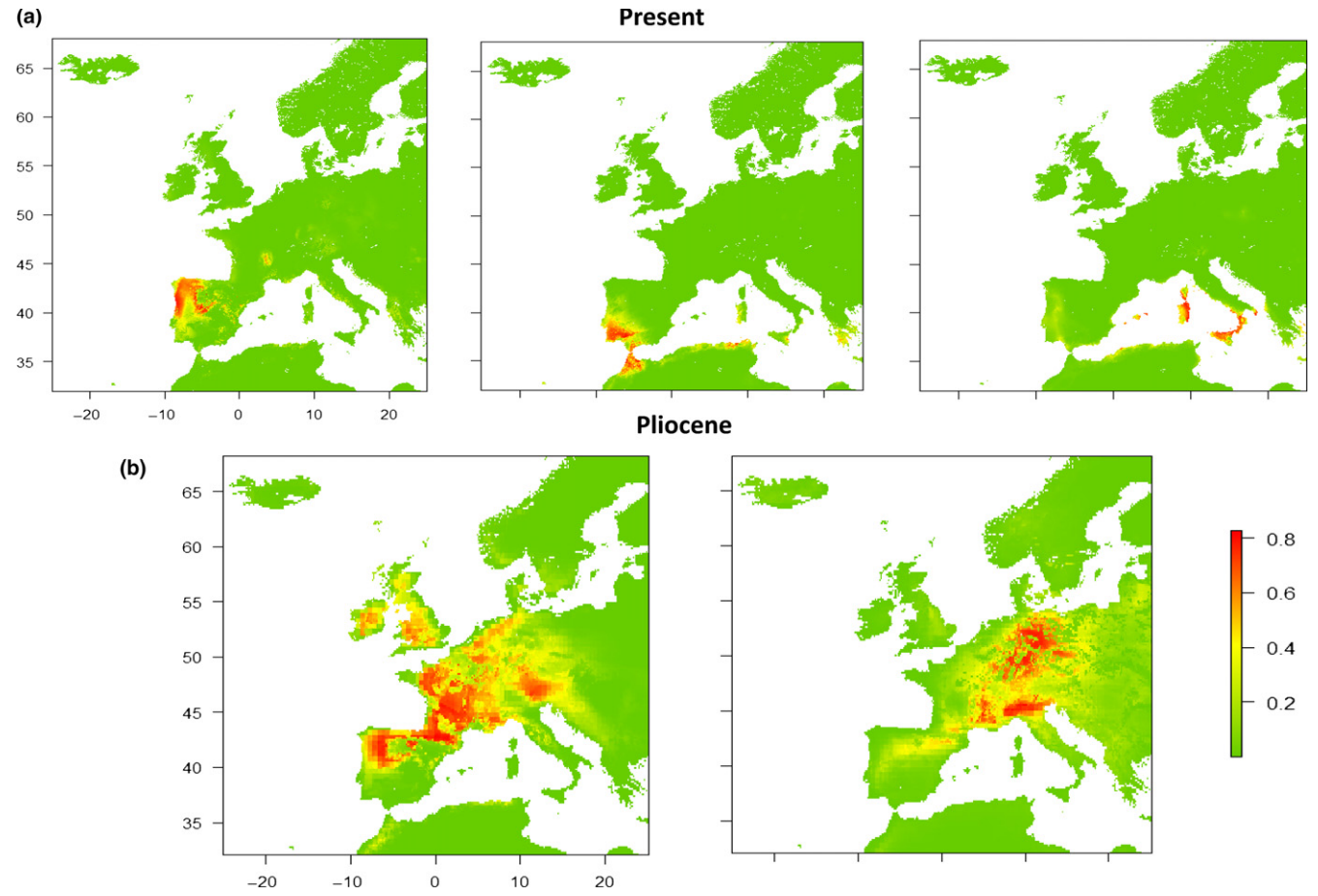

FIGURE 4 Climatic suitability and potential distributions (a) at present as predicted by MAXENT (Phillips, Anderson, & Schapire, 2006) for, from left to right: *Carex reuteriana* ssp. *reuteriana*, ssp. *mauritanica* and *Carex panormitana*. (b) The left plot shows the distribution projected for the species complex (*C. reuteriana*–*C. panormitana*) at the middle Pliocene (3 Ma) with a model calibrated with present occurrences, and the right plot displays the potential distribution of the species complex at the middle Pliocene according to the model calibrated with fossil records [Colour figure can be viewed at wileyonlinelibrary.com]

Netherlands), where the fossil record supports its presence during the Pliocene (Jiménez-Mejías et al., 2016).

The genetic pattern from AFLP variation (Figure 2) and genealogical relationships of nuclear haplotypes (Figure S2b) revealed a clear genetic differentiation between both species. The formation of genetic clusters of populations within each taxon according to disjunct areas, together with the almost complete absence of genetic admixture between them (Figure 2), points to lack of gene flow between them due to geographical barriers and thus to allopatric differentiation (Figures 2 and 3b). Furthermore, *C. panormitana* shows a strong differentiation between the Sardinian and the Sicilian–Tunisian populations (Figure 2; but see haplotype network, Figure S2a,b). The closer relationships between North African-Sicilian populations than between Sicilian–Sardinian ones was previously suggested in other Mediterranean endemic plant groups (De Castro, Véla, Vendramin, Gargiulo, & Caputo, 2015; Zitari et al., 2011).

Therefore, our results support vicariance as the more plausible explanation for the current distribution range of *C. reuteriana*–*C. panormitana*. The current patchy distribution would be the result of the split of a more continuous past range in Europe into at least two putative refugial areas during the Middle Pleistocene. One of them was probably situated in the western Mediterranean and another in the central Mediterranean (Table 2b; Figure 3b). The populations of each of these refugia derived into the two extant species, respectively, *C. reuteriana* and *C. panormitana*. In addition, the split between these two species as sisters, together with the fossil record supporting the presence of its putative ancestor (*C. panormitana*-like plants) in the Tyrrhenian (now mainland Italy) during the early Pliocene (Figure 1), also excludes the possibility of a west–east migration in the Mediterranean Basin.

4.2 | Historical niche evolution from Pliocene to present

Although diversification in the Mediterranean is often associated with frequent niche shifts (Donoghue, 2008; Rundel et al., 2016), our study presents a case of a group diversified in the Mediterranean with more complex niche dynamics. The ecological history of the group is characterized by an initial niche shift from the milder, less seasonal, Pliocenic conditions to the harsher Pleistocene ones

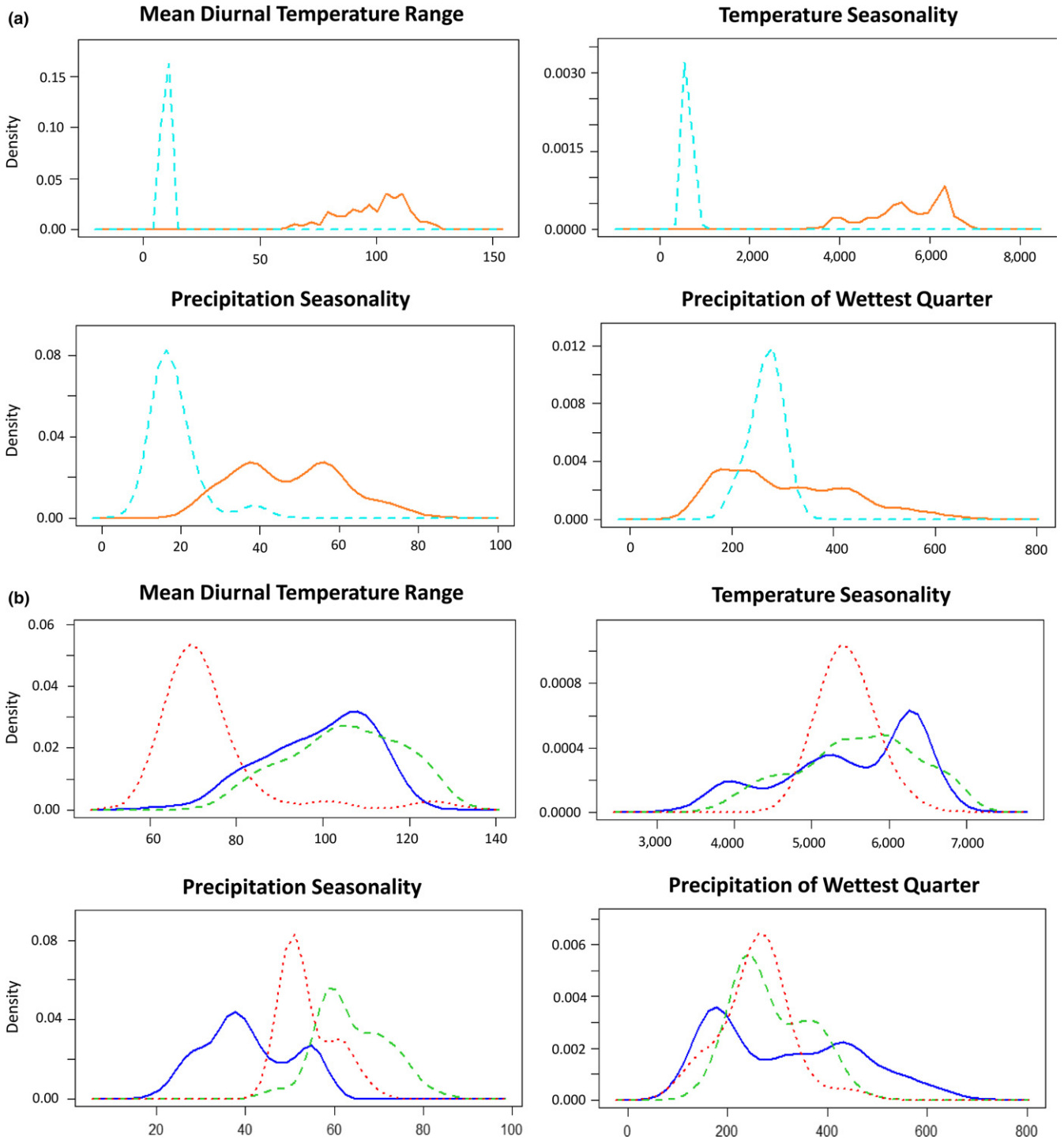

FIGURE 5 Comparison of fitted responses to the four bioclimatic variables of (a) extant species complex (continuous line) vs. Pliocene *Carex panormitana*-type fossils (dashed line), and (b) extant taxa only (dashed line represents *Carex reuteriana* ssp. *mauritanica*, continuous line ssp. *reuteriana*, and dotted line *C. panormitana*). Colours are as in Figure 1, except for all populations of *C. panormitana* which are displayed in red [Colour figure can be viewed at wileyonlinelibrary.com]

(Figures 5a and 6). Afterwards, however, the bioclimatic niche appears more conserved during the diversification of the group through the Pleistocene to the present, with only minor local adaptations (Table 3; Figures 5b and 6).

The broad suitable areas projected in central Europe for the Pliocene (both based on extant and fossil occurrences; Figure 4) contrast strongly with the current distribution restricted to the western Mediterranean Basin (Figure 1). This historical southwards range shift, parallel to the deterioration of climatic conditions between the Pliocene and the present (cooler and more seasonal climates), can explain the significantly different niches found for the Pliocene ancestor and current taxa (Table 3; Figure 6). This niche

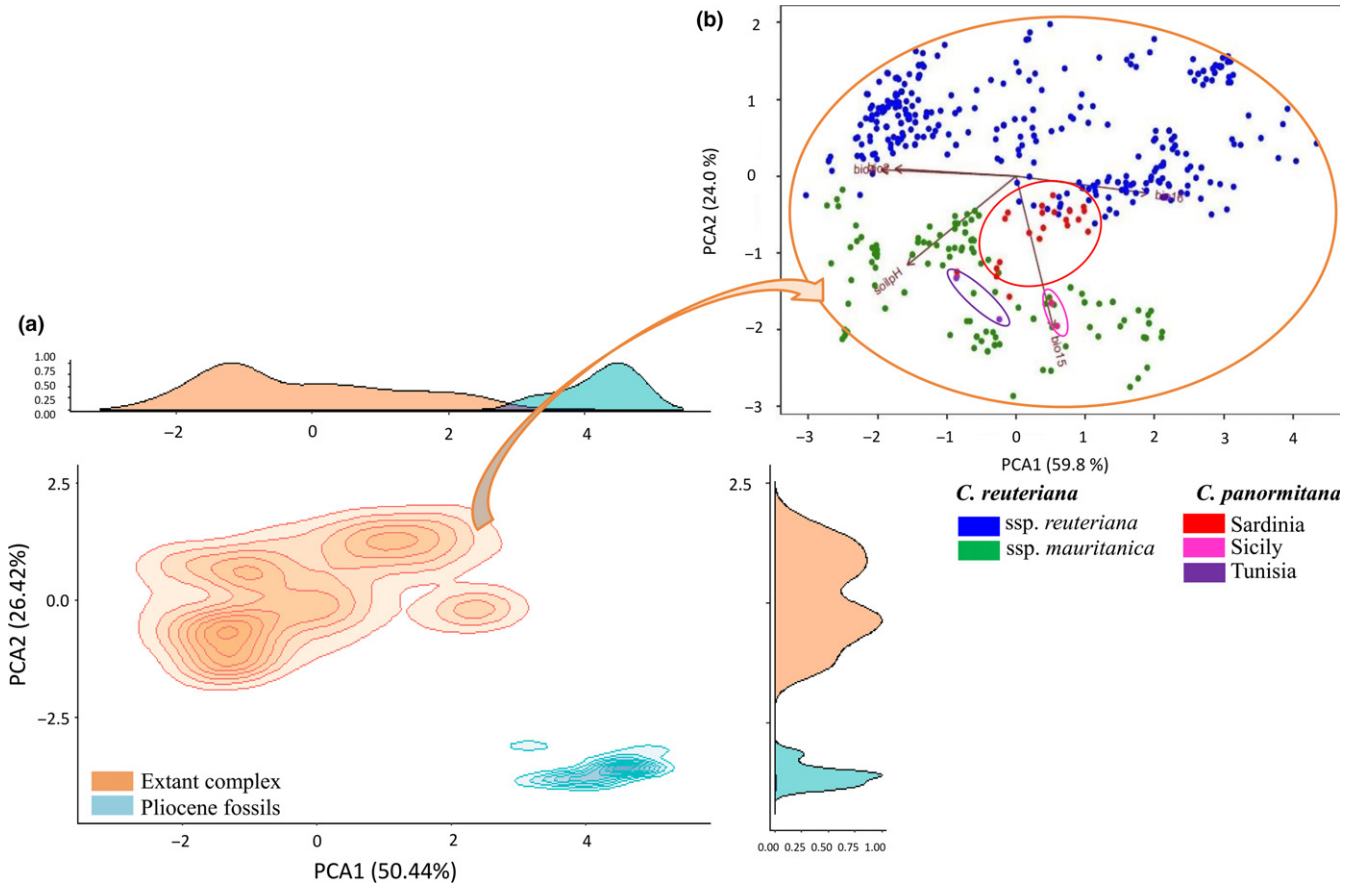

FIGURE 6 Differences in the environmental niche of extant and fossil populations of *Carex reuteriana–Carex panormitana* species complex. Both plots depict the population values in an environmental space defined by the first two axes from a principal components analysis (PCA) of the four bioclimatic variables (see Figure 5) and soil pH. (a) Comparison of *C. reuteriana–C. panormitana* extant complex (orange) and their Pliocene fossil ancestor; (b) comparison of populations of the extant species complex; coloured dots represent the different taxa/population groups according to the retrieved genetic structure [Colour figure can be viewed at wileyonlinelibrary.com]

TABLE 3 Pairwise statistical test for comparison of ecological niche overlap between the different genetic and taxonomic groups that compose the current complex, so as with its fossil ancestor

Hypotheses: "The niche overlap is more similar/equivalent than at random"	Numbers of populations (*N*)	Schoener's D	Niche similarity (1->2) *p*	Niche similarity (2->1) *p*	Niche equivalency *p*
Among groups					
Complex vs. fossils	462/17	0	1	1	-
Carex reuteriana vs. *C. panormitana*	433/29	0.193	0.129	0.139	0.525
C. reuteriana ssp. *reuteriana* vs. ssp. *mauritanica*	315/118	0.095	0.04	0.04	1
C. panormitana Sicilian–Tunisian vs. Sardinian populations	8/21	0.169	0.14	0.158	0.604

Their statistical significance is represented by *p*-values (Warren et al., 2008).

shift might be associated with the Plio–Pleistocene transition and the onset of the Mediterranean climate (c. 3.2 Ma, Suc et al., 1995), which would promote adaptation to the seasonally drier new climate (e.g., Mairal et al., 2017). In contrast, niche differentiation of disjunctive species after the speciation event (i.e., Late Pleistocene) seems to have been much weaker (Table 3; Figure 5b). Whereas the relatively similar environmental niches after the speciation event (Wiens & Graham, 2005; Wiens et al., 2010) would support the PNC hypothesis (Crisp & Cook, 2012; Donoghue, 2008; Mairal et al., 2017), there is also some differentiation in the occupied environments among extant species, which could be related to local adaptation processes.

A certain degree of ecological divergence seems to have taken place at a finer evolutionary level at least within *C. reuteriana*, as the ecological niche obtained for both subspecies was mostly different in their allopatric ranges (Figures 1 and 6). While ssp. *reuteriana* is associated with a more oceanic climate, ssp. *mauritanica* inhabits more Mediterranean conditions (Figure 5b). This suggests that ecological constraints acting upon populations do not depend so much on the species intrinsic characteristics, but on the local conditions of the geographic region where they are distributed (Boucher-Lalonde, Morin, & Currie, 2016), which in turn promote the geographic isolation and the subsequent genetic structure (Cavender-Bares & Pahlich, 2009; Hosseinian Yousefkhani, Rastegar-Pouyani, & Aliabadian, 2016). The presence of geographical barriers that limited expansion (Wiens, 2004a), as well as microhabitat preferences (Thompson, 2005) may have also played a role.

The PNC is usually associated with the concept of ecological vicariance (Crisp & Cook, 2012; Wiens & Graham, 2005) resulting in different lineages that present similar ecological traits in different parts of a same geographical region. The disjunct distribution pattern of *C. reuteriana*–*C. panormitana* could be in agreement with a scenario of ecological vicariance if the hypothetical Mediterranean common ancestor of the two species already had ecological requirements similar to those of the lineages resulting after the Pleistocene speciation process. This is supported by the results from the SDM and comparison of ecological niche analyses (Table 3; Figures 4 and S3). Evidence for ecological vicariance in this area has been reported in previous studies (cf. Mairal et al., 2017; Martín-Bravo & Escudero, 2012). During the Pleistocene, the more continuous range of their last common ancestor was fragmented by the changing climatic conditions, and the resulting populations were confined to areas which harboured suitable habitats during the Pleistocene glaciation cycles (at least from the LIG; Figure S3).

4.3 | Concluding remarks

Our results establish a clear geography-based genetic differentiation between *C. reuteriana* and *C. panormitana*. The ecological niche dynamics of this species complex could be linked to the current distribution range in isolated patches in the Mediterranean. Thus, two different strategies through time were inferred: (i) a first niche shift from the milder central European Pliocene climate to the seasonally dry Mediterranean, potentially involving an adaptive response to the changing environmental conditions; and (ii) much weaker niche differentiation during the Pleistocene, probably associated with local adaptation processes (i.e., ecological differentiation at the intraspecific level). This stronger niche conservatism could have produced range shifts during glaciation cycles to accommodate to climatically suitable areas (ecological vicariance). This study thus rejects the hypothesis of diversification involving frequent niche shifts in the Mediterranean Basin, and displays a more complex scenario where both niche shift and conservatism may have had a relevant role in the evolutionary and biogeographic history of Mediterranean plants.

The integrative approach followed in this study, combining phylogenetics, phylogeography, ecological niche comparison, distribution modelling, and considering the known fossil record of the group, allows innovative and robust inferences regarding species' response to climatic changes in a dynamic geological–environmental setting. The synergy of integrating alternative data sources may be the key to face similar challenging evolutionary questions in other taxonomic groups or geographical regions.

ACKNOWLEDGEMENTS

This work was carried out with financial support by the Spanish Ministry of Economy and Competitiveness (project CGL2016-77401-P), F.R.S. was supported by a postdoctoral fellowship from the same Ministry (FPD-2013-16756), and C.B.B. by a Predoctoral Fellowship Program grant from the Ministry of Education, Culture and Sports (FPU16/01257). The authors wish to thank two anonymous reviewers that contributed to improve the quality of our paper with their comments; Professors M. Luceño and P. Vargas for their support and advise; M. Urbani, D. Cusimano and G.E. Rodríguez for providing essential plant material for the study; the curators and staff of COFC, SEV, SS, M and UPOS herbaria for granting us to access to their collections and for providing plant material; and M. Míguez (UPOS) for technical support. We also thank Andalusian Scientific Information Technology Center (CICA, Seville, Spain) for providing computational resources.

DATA ACCESSIBILITY

Obtained DNA sequences for studied regions are available in NCBI GenBank (see Appendix S1) and DRYAD repository (see Appendix S3; http://datadryad.org/review?doi=doi:10.5061/dryad.76tk7).

AUTHOR CONTRIBUTION

P.J.-M. and S.M.-B. conceived the idea; P.J.-M. and M.E. collected plant material; C.B.-B., P.J.-M. and S.M.-B. carried out the laboratory work; C.B.-B., P.J.-M., S.M.-B. and M.E. analysed the data, assisted by F.R.S. for the ecological niche analyses; C.B.-B., P.J.-M. and S.M.-B. led the drafting of the manuscript; all authors contributed to the preparation of the final version.

ORCID

C. Benítez-Benítez http://orcid.org/0000-0003-4956-0343
M. Escudero http://orcid.org/0000-0002-2541-5427
F. Rodríguez-Sánchez http://orcid.org/0000-0002-7981-1599
S. Martín-Bravo http://orcid.org/0000-0003-0626-0770
P. Jiménez-Mejías http://orcid.org/0000-0003-2815-4477

REFERENCES

Ackerly, D. D. (2003). Community assembly, niche conservatism, and adaptive evolution in changing environments. *International Journal of Plant Sciences*, *164*, 165–184. https://doi.org/10.1086/368401

Anacker, B. L., & Strauss, S. Y. (2014). The geography and ecology of plant speciation: Range overlap and niche divergence in sister species. *Proceedings of the Royal Society*, *281*, 20132980. https://doi.org/10.1098/rspb.2013.2980

Ball, P. W., & Reznicek, A. A. (2002). Carex [Generic description and key to species]. In Flora of North America Editorial Committee (Eds.), *Flora of North America*, Vol. 23 (pp. 254–273). New York, NY and Oxford, UK: Oxford University Press.

Bonin, A., Bellemain, A. E., Bronken Eidesen, P., Pompanon, F., Brochmann, C., & Taberlet, P. (2004). How to track and assess genotyping errors in population genetic studies. *Molecular Ecology*, *13*, 3261–3273. https://doi.org/10.1111/j.1365-294X.2004.02346.x

Boucher-Lalonde, V., Morin, A., & Currie, D. J. (2016). Can the richness-climate relationship be explained by systematic variations in how individual species' ranges relate to climate? *Global Ecology and Biogeography*, *25*, 527–539. https://doi.org/10.1111/geb.12433

Bouckaert, R., Heled, J., Kühnert, D., Vaughan, T., Wu, C. H., Xie, D., … Drummond, A. J. (2014). BEAST 2: A software platform for Bayesian evolutionary analysis. *PloS Computational Biology*, *10*, e1003537. https://doi.org/10.1371/journal.pcbi.1003537.g002

Broennimann, O., Fitzpatrick, M. C., Pearman, P. B., Petitpierre, B., Pellissier, L., Yoccoz, N. G., & Guisan, A. (2012). Measuring ecological niche overlap from occurrence and spatial environmental data. *Global Ecology and Biogeography*, *21*, 481–497. https://doi.org/10.1111/j.1466-8238.2011.00698.x

Broennimann, O., Treier, U. A., Muller-Scharer, H., Thuiller, W., Peterson, A. T., & Guisan, A. (2007). Evidence of climatic niche shift during biological invasion. *Ecology Letters*, *10*, 701–709. https://doi.org/10.1111/j.1461-0248.2007.01060.x

Brummitt, R. K. (2001). *World geographical scheme for recording plant distributions*, 2nd ed. Pittsburgh, Pennsylvania, USA: Hunt Institute for Botanical Documentation, Carnegie Mellon University.

Bryant, D., Bouckaert, R., Felsenstein, J., Rosenberg, N. A., & Roy Choudhury, A. (2012). Inferring species trees directly from biallelic genetic markers: By passing gene trees in a full coalescent analysis. *Molecular Biology and Evolution*, *29*, 1917–1932. https://doi.org/10.1093/molbev/mss086

Cavender-Bares, J., & Pahlich, A. (2009). Molecular, morphological, and ecological niche differentiation of sympatric sister oak species, *Quercus virginiana* and *Q. geminata* (Fagaceae). *American Journal of Botany*, *96*, 1690–1702. https://doi.org/10.3732/ajb.0800315

Clement, M., Posada, D., & Crandall, K. (2000). TCS: A computer program to estimate gene genealogies. *Molecular Ecology*, *9*, 1657–1660. https://doi.org/10.1046/j.1365-294x.2000.01020.x

Crisp, M. D., Arroyo, M. T. K., Cook, L. G., Gandolfo, M. A., Jordan, G. J., McGlone, M. S., … Linder, H. P. (2009). Phylogenetic biome conservatism on a global scale. *Letters*, *458*, 754–756.

Crisp, M. D., & Cook, L. G. (2012). Phylogenetic niche conservatism: What are the underlying evolutionary and ecological causes? *New Phytologist*, *196*, 681–694. https://doi.org/10.1111/j.1469-8137.2012.04298.x

Darriba, D., Taboada, G. L., Doallo, R., & Posada, D. (2012). JModelTest 2: More models, new heuristics and parallel computing. *Nature Methods*, *9*, 772. https://doi.org/10.1038/nmeth.2109

Darwin, C. (1859). *On the origin of species*. London: J. Murray.

De Castro, O., Véla, E., Vendramin, G. G., Gargiulo, R., & Caputo, P. (2015). Genetic structure in the *Genista ephedroides* complex (Fabaceae) and implications for its present distribution. *Botanical Journal of the Linnean Society*, *177*, 607–618. https://doi.org/10.1111/boj.12263

Di Cola, V., Broennimann, O., Petitpierre, B., Breiner, F. T., D'Amen, M., Randin, C., … Pellissier, L. (2017). Ecospat: An R package to support spatial analyses and modeling of species niche and distributions. *Ecography*, *40*, 774–787. https://doi.org/10.1111/ecog.02671

Donoghue, M. J. (2008). A phylogenetic perspective on the distribution of plant diversity. *Proceedings of the National Academy of Sciences*, *105*, 11549–11555. https://doi.org/10.1073/pnas.0801962105

Dragon, J., & Barrington, D. S. (2009). Systematics of the *Carex aquatilis* and *C. lenticularis* lineages: Geographically and ecologically divergent sister clades of *Carex* section *Phacocystis* (Cyperaceae). *American Journal of Botany*, *96*, 1896–1906. https://doi.org/10.3732/ajb.0800404

Drummond, A. J., & Rambaut, A. (2007). BEAST: Bayesian evolutionary analysis by sampling trees. *BMC Evolutionary Biology*, *7*, 214. https://doi.org/10.1186/1471-2148-7-214

Drummond, A. J., Suchard, M. A., Xie, D., & Rambaut, A. (2012). Bayesian Phylogenetics with BEAUti and the BEAST 1.7. *Molecular Biology & Evolution*, *29*, 1969–1973. https://doi.org/10.1093/molbev/mss075

Earl, D. A., & VonHoldt, B. M. (2012). STRUCTURE HARVESTER: A website and program for visualizing STRUCTURE output and implementing the Evanno method. *Conservation Genetics Resources*, *4*, 359–361. https://doi.org/10.1007/s12686-011-9548-7

Edgar, R. C. (2004). MUSCLE: Multiple sequence alignment with high accuracy and high throughput. *Nucleic Acids Research*, *32*, 1792–1797. https://doi.org/10.1093/nar/gkh340

Elith, J., Phillips, S. J., Hastie, T., Dudík, M., Chee, Y. E., & Yates, C. J. (2011). A statistical explanation of MaxEnt for ecologists. *Diversity and Distributions*, *17*, 43–57. https://doi.org/10.1111/j.1472-4642.2010.00725.x

Evans, M. E. K., Smith, S. A., Flynn, R. S., & Donoghue, M. J. (2009). Climate, Niche evolution, and Diversification of the "Bird-Cage" Evening Primroses (*Oenothera*, Sections *Anogra* and *Kleinia*). *American Society of Naturalists*, *173*, 225–240. https://doi.org/10.1086/595757

Fernández-Mazuecos, M., Blanco-Pastor, J. L., & Vargas, P. (2013). A phylogeny of toadflaxes (*Linaria* Mill.) based on nuclear internal transcribed spacer sequences: Systematic and evolutionary consequences. *International Journal of Plant Sciences*, *174*, 234–249. https://doi.org/10.1086/668790

Fernández-Mazuecos, M., Jiménez-Mejías, P., Martín-Bravo, S., Buide, M. L., Álvarez, I., & Vargas, P. (2016). Narrow endemics on coastal plains: Miocene divergence of the critically endangered genus *Avellara* (Compositae). *Plant Biology*, *18*, 729–738. https://doi.org/10.1111/plb.12458

Fiz-Palacios, O., & Valcárcel, V. (2013). From Messinian crisis to Mediterranean climate: A temporal gap of diversification recovered from multiple plant phylogenies. *Perspectives in Plant Ecology, Evolution and Systematics*, *15*, 130–137. https://doi.org/10.1016/j.ppees.2013.02.002

Gentili, R., Bacchetta, G., Fenu, G., Cogoni, D., Abeli, T., Rossi, G., … Citterio, S. (2015). From cold to warm-stage refugia for boreo-alpine plants in southern European and Mediterranean mountains: The last chance to survive or an opportunity for speciation? *Biodiversity*, *16*, 247–261. https://doi.org/10.1080/14888386.2015.1116407

Gianguzzi, L., Cusimano, D., Ilardi, V., & Salvatore, R. (2013). Distribution, ecology, vegetation and conservation survey on the relictual population of *Carex panormitana* Guss. (Cyperaceae) in Sicily (Italy). *Webbia, Journal of Plant Taxonomy and Geography*, *68*, 159–175.

Global Carex Group (2016). Megaphylogenetic specimen-level approaches to the *Carex* (Cyperaceae) phylogeny using regions ITS, ETS, and matK: Implications for classification. *Systematic Botany*, *41*, 500–518.

González-Martínez, S. C., Dubreuil, M., Riba, M., Vendramin, G. G., Sebastiani, F., & Mayol, M. (2010). Spatial genetic structure of *Taxus baccata* L. in the western Mediterranean Basin: Past and present limits to gene movement over a broad geographic scale. *Molecular Phylogenetics & Evolution*, *55*, 805–815. https://doi.org/10.1016/j.ympev.2010.03.001

Grafen, A. (1989). The phylogenetic regression. *Philosophical Transactions of the Royal Society of London, Series B: Biological Sciences*, *326*, 119–157. https://doi.org/10.1098/rstb.1989.0106

Harvey, P. H., & Pagel, M. D. (1991). *The comparative method in evolutionary biology*. Oxford, UK: Oxford University Press.

Heiberger, R. M. (2017). HH: Statistical analysis and data display: Heiberger and Holland. R package v. 3.1-34. https://CRAN.R-project.org/package=H

Hey, J. (2010). Isolation with Migration Models for more than two populations. *Molecular Biology and Evolution*, *27*, 905–920. https://doi.org/10.1093/molbev/msp296

Hijmans, R. J., Cameron, S. E., Parra, J. L., Jones, P. G., & Jarvis, A. (2005). Very high resolution interpolated climate surfaces for global land areas. *International Journal of Climatology*, *25*, 1965–1978. https://doi.org/10.1002/(ISSN)1097-0088

Holt, R. D. (1996). Demographic constraints in evolution: Towards unifying the evolutionary theories of senescence and niche conservatism. *Evolutionary Ecology*, *10*, 1–11. https://doi.org/10.1007/bf01239342

Hosseinian Yousefkhani, S. S., Rastegar-Pouyani, E., & Aliabadian, M. (2016). Ecological niche differentiation and taxonomic distinction between *Eremias strauchi strauchi* and *Eremias strauchi kopetdaghica* (Squamata: Lacertidae) on the Iranian Plateau based on ecological niche modeling. *Italian Journal of Zoology*, *83*, 408–416. https://doi.org/10.1080/11250003.2016.1209581

Janes, J. K., Miller, J. M., Dupuis, J. R., Malenfant, R. M., Gorrell, J. C., Cullingham, C. I., & Andrew, R. L. (2017). The K = 2 conundrum. *Molecular Ecology*, *26*, 3594–3602. https://doi.org/10.1111/mec.14187

Jara-Arancio, P., Arroyo, M. T. K., Guerrero, P. C., Hinojosa, L. F., Arancio, G., & Méndez, M. A. (2014). Phylogenetic perspectives on biome shifts in *Leucocoryne* (Alliaceae) in relation to climatic niche evolution in western South America. *Journal of Biogeography*, *41*, 328–338. https://doi.org/10.1111/jbi.12186

Jiménez-Mejías, P. (2011). *Taxonomía y Sistemática de las secciones Ceratocystis y Phacocystis del género Carex en Europa y la cuenca mediterránea* (Tesis doctoral). Sevilla, Spain: Universidad Pablo de Olavide.

Jiménez-Mejías, P., Escudero, M., Chaparro, A. J., & Luceño, M. (2007). Novedades corológicas del genero *Carex* para la Peninsula Iberica. *Acta Botanica Malacitana*, *32*, 305–309.

Jiménez-Mejías, P., Escudero, M., Guerra-Cárdenas, S., Lye, K. A., & Luceño, M. (2011). Taxonomic delimitation and drivers of speciation in the Ibero-North African *Carex* sect. *Phacocystis* river-shore group (Cyperaceae). *American Journal of Botany*, *11*, 1855–1867. https://doi.org/10.3732/ajb.1100120

Jiménez-Mejías, P., Fernández-Mazuecos, M., Amat, M. E., & Vargas, P. (2015). Narrow endemics in European mountains: High genetic diversity within the monospecific genus *Pseudomisopates* (Plantaginaceae) despite isolation since the late Pleistocene. *Journal of Biogeography*, *42*, 1455–1468. https://doi.org/10.1111/jbi.12507

Jiménez-Mejías, P., & Luceño, M. (2011). *Euro + Med Plantbase. The information resource for Euro-Mediterranean plant diversity*. Retrieved from http://ww2.bgbm.org/EuroPlusMed/query.asp

Jiménez-Mejías, P., Martín-Bravo, S., Amini-Rad, M., & Luceño, M. (2013). Disentangling the taxonomy of Carex acuta s.l. in the Mediterranean Basin and the Middle East: Re-evaluation of C. panormitana Guss. and C. kurdica Kük. ex Hand.-Mazz. *Plant Biosystem*, *148*, 64–73.

Jiménez-Mejías, P., & Martinetto, E. (2013). Toward an accurate taxonomic interpretation of Carex fossil fruits (Cyperaceae): A case study in section Phacocystis in the Western Palearctic. *American Journal of Botany*, *100*, 1580–1603. https://doi.org/10.3732/ajb.1200629

Jiménez-Mejías, P., Martinetto, E., Momohara, A., Popova, S., Smith, S. Y., & Roalson, E. H. (2016). A commented synopsis of the pre-Pleistocene fossil record of *Carex* (Cyperaceae). *The Botanical Review*, *82*, 258–345. https://doi.org/10.1007/s12229-016-9169-7

Koecke, A. V., Muellner-Riehl, A. N., Pennington, T. D., Schorr, G., & Schnitzler, J. (2013). Niche evolution through time and across continents: The story of Neotropical *Cedrela* (Meliaceae). *American Journal of Botany*, *100*, 1800–1810. https://doi.org/10.3732/ajb.1300059

Lavergne, S., Mouquet, N., Thuiller, W., & Ronce, O. (2010). Biodiversity and climate change: Integrating evolutionary and ecological responses of species and communities. *Annual Reviews*, *41*, 321–350.

Librado, P., & Rozas, J. (2009). DnaSP v5: Software for comprehensive analysis of DNA polymorphism data. *Bioinformatics*, *25*, 1451–1452. https://doi.org/10.1093/bioinformatics/btp187

Lima-Ribeiro, M. S., Varela, S., González-Hernández, J., Oliveira, G., Diniz-Filho, J. A. F., & Terribile, L. C. (2015). ecoClimate: A database of climate data from multiple models for past, present, and future for Macroecologists and Biogeographers. *Biodiversity Informatics*, *10*, 1–21.

Losos, J. B. (2008). Phylogenetic niche conservatism, phylogenetic signal and the relationship between phylogenetic relatedness and ecological similarity among species. *Ecology Letters*, *11*, 995–1007. https://doi.org/10.1111/j.1461-0248.2008.01229.x

Luceño, M., & Jiménez-Mejías, P. (2008). *Carex* (Cyperaceae). In S. Castroviejo, et al. (Eds.), *Flora Iberica. Plantas vasculares de la Península Ibérica e Islas Baleares*, Vol. *18* (pp. 109–250). Madrid: Real Jardín Botánico, CSIC.

Maguilla, E., Escudero, M., Waterway, M. J., Hipp, A. L., & Luceño, M. (2015). Phylogeny, Systematics, and trait evolution of *Carex* section *Glaerosae*. *American Journal of Botany*, *102*, 1–17.

Mairal, M., Sanmartín, I., & Pellissier, L. (2017). Lineage-specific climatic niche drives the tempo of vicariance in the Rand Flora. *Journal of Biogeography*, *44*, 911–923. https://doi.org/10.1111/jbi.12930

Mansion, G., Rosenbaum, G., Schoenenberger, N., Bacchetta, G., Rosselló, J. A., & Conti, E. (2008). Phylogenetic analysis informed by geological history supports multiple, sequential invasions of the Mediterranean Basin by the angiosperm family Araceae. *Systematic Biology*, *57*, 269–285. https://doi.org/10.1080/10635150802044029

Martín-Bravo, S., & Escudero, M. (2012). Biogeography of flowering plants: A case study in mignonettes (Resedaceae) and sedges. (*Carex*, Cyperaceae). *Global Advances in Biogeography 13*, 257–290.

Médail, F., & Diadema, K. (2009). Glacial refugia influence plant diversity patterns in the Mediterranean Basin. *Journal of Biogeography*, *36*, 1333–1345. https://doi.org/10.1111/j.1365-2699.2008.02051.x

Médail, F., & Quézel, P. (1997). Hot-spots analysis for conservation of plant biodiversity in the Mediterranean Basin. *Annals of the Missouri Botanical Garden*, *84*, 112–127. https://doi.org/10.2307/2399957

Merow, C., Smith, M. J., & Silander, J. A. Jr. (2013). A practical guide to MaxEnt for modeling species' distributions: What it does, and why inputs and settings matter. *Ecography*, *36*, 1058–1069. https://doi.org/10.1111/j.1600-0587.2013.07872.x

Míguez, M., Gehrke, B., Maguilla, E., Jiménez-Mejías, P., & Martín-Bravo, S. (2017). *Carex* sect. *Rhynchocystis* (Cyperaceae): A Tertiary subtropical relict in the western Palearctic showing a dispersal derived Rand-Flora Pattern. *Journal of Biogeography*, *44*, 2211–2224. https://doi.org/10.1111/jbi.13027

Milne, R. I., & Abbott, R. J. (2002). The origin and evolution of tertiary relict floras. *Advances in Botanical Research*, *38*, 281–314. https://doi.org/10.1016/S0065-2296(02)38033-9

Mod, H. K., Scherrer, D., Luoto, M., & Guisan, A. (2016). What we use is not what we know: Environmental predictors in plant distribution models. *Journal of Vegetation Science*, *27*, 1308–1322. https://doi.org/10.1111/jvs.12444

Münkemüller, T., Boucher, F. C., Thuiller, W., & Lavergne, S. (2015). Phylogenetic niche conservatism-common pitfalls and ways forward. *Functional Ecology*, *29*, 627–639. https://doi.org/10.1111/1365-2435.12388

Myers, N., Mittermeier, R. A., Mittermeier, C. G., da Fonseca, G. A. B., & Kent, J. (2000). Biodiversity hotspots for conservation priorities. *Nature*, *403*, 853–858. https://doi.org/10.1038/35002501

Peakall, R., & Smouse, P. E. (2012). GenAlEx 6.5: Genetic analysis in Excel. Population genetic software for teaching and research-an

update. *Bioinformatics*, *28*, 2537–2539. https://doi.org/10.1093/bioinformatics/bts460

Pettengill, J. B., & Moeller, D. A. (2012). Phylogeography of speciation: Allopatric divergence and secondary contact between outcrossing and selfing *Clarkia*. *Molecular Ecology*, *21*, 4578–4592. https://doi.org/10.1111/j.1365-294X.2012.05715.x

Phillips, S. J., Anderson, R. P., Dudík, M., Schapire, R. E., & Blair, M. E. (2017). Opening the black box: An open-source release of Maxent. *Ecography*, *40*, 887–893. https://doi.org/10.1111/ecog.03049

Phillips, S. J., Anderson, R. P., & Schapire, R. E. (2006). Maximum entropy modeling of species geographic distributions. *Ecological Modelling*, *190*, 231–259. https://doi.org/10.1016/j.ecolmodel.2005.03.026

Pignatti, S. (1982). *Flora d'Italia*. Bologna, Italy: Edagricole.

Pritchard, J. K., Stephens, M., & Donnelly, P. (2000). Inference of population structure using multilocus genotype data. *Genetics*, *155*, 945–959.

Qiu, Y. X., Qi, X. S., Jin, X. F., Tao, X. Y., Fu, C. X., Naiki, A., & Comes, H. P. (2009). Population genetic structure, phylogeography, and demographic history of *Platycrater arguta* (Hydrangeaeae) endemic to East China and South Japan, inferred from chloroplast DNA sequence variation. *Taxon*, *58*, 1226–1241.

R Development Core Team. (2017). *R: A language and environment for statistical computing*. Vienna, Austria: R Foundation for Statistical Computing. Retrieved from https://www.r-project.org/

Ramasamy, R. K., Ramasamy, S., Bindroo, B. B., & Naik, V. G. (2014). STRUCTURE PLOT: A program for drawing elegant STRUCTURE bar plots in user friendly interface. SpringerPlus, https://doi.org/10.1186/2193-1801-3-431

Rambaut, A. (2012). FigTree, tree figure drawing tool v. 1.4.0. Retrieved from http://tree.bio.ed.ac.uk/software/figtree/

Rambaut, A., & Drummond, A. J. (2014). Tracer v. 1.6. Retrieved from http://beast.bio.ed.ac.uk/Tracer

Revell, L. J., Harmon, L. J., & Collar, D. C. (2008). Phylogenetic signal, evolutionary process, and rate. *Systematic Biology*, *57*, 591–601. https://doi.org/10.1080/10635150802302427

Rodríguez-Sánchez, F., Pérez-Barrales, R., Ojeda, F., Vargas, P., & Arroyo, J. (2008). The Strait of Gibraltar as a melting pot for plant biodiversity. *Quaternary Science Reviews*, *27*, 2100–2117. https://doi.org/10.1016/j.quascirev.2008.08.006

Rundel, P. W., Arroyo, M. T. K., Cowling, R. M., Keeley, J. E., Lamont, B. B., & Vargas, P. (2016). Mediterranean biomes: Evolution of their vegetation, floras, and climate. *Annual Review of Ecology, Evolution and Systematics*, *47*, 383–407. https://doi.org/10.1146/annurev-ecolsys-121415-032330

Schoener, T. W. (1968). Anolis lizards of Bimini: Resource partitioning in a complex fauna. *Ecology*, *49*, 704–726. https://doi.org/10.2307/1935534

Shaw, J., Lickey, E. B., Beck, J. T., Farmer, S. B., Liu, W., Miller, J., … Small, R. L. (2005). The tortoise and the Hare II: Relative utility of 21 noncoding chloroplast DNA sequences for phylogenetic analysis. *American Journal of Botany*, *92*, 142–166. https://doi.org/10.3732/ajb.92.1.142

Shaw, J., Lickey, E. B., Schilling, E. E., & Small, R. L. (2007). Comparison of whole chloroplast genome sequences to choose noncoding regions for phylogenetic studies in angiosperms: The Tortoise and the Hare III. *American Journal of Botany*, *94*, 275–288. https://doi.org/10.3732/ajb.94.3.275

Spalink, D., Drew, B. T., Pace, M. C., Zaborsky, J. G., Li, P., Cameron, K. M., … Sytsma, K. J. (2016). Evolution of geographical place and niche space: Patterns of diversification in the North American sedge (Cyperaceae) flora. *Molecular Phylogenetics and Evolution*, *95*, 183–195. https://doi.org/10.1016/j.ympev.2015.09.028

Stiels, D., Gaißer, B., Schidelko, K., Engler, J. O., & Rödder, D. (2015). Niche shift in four nonnative estrildid finches and implications for species distribution models. *Ibis*, *157*, 75–90. https://doi.org/10.1111/ibi.12194

Suc, J. P., Bertini, A., Combourieu-Nebout, N., Diniz, F., Leroy, S., Russo-Ermolli, E., … Ferrier, J. (1995). Structure of West Mediterranean vegetation and climate since 5.3 ma. *Acta Zoologica Cracova*, *38*, 3–16.

Swets, J. A. (1988). Measuring the accuracy of diagnostic systems. *Science*, *240*, 1285. https://doi.org/10.1126/science.3287615

Swofford, D. L. (2002). *PAUP*: Phylogenetic analysis using parsimony (and other methods) v. 4.0b10*. Sunderland, Massachusetts, USA: Sinauer. https://doi.org/10.1111/j.0014-3820.2002.tb00191

Taberlet, P., Fumagalli, L., Wust-Saucy, A. G., & Cosson, J. F. (1998). Comparative phylogeography and postglacial colonisation routes in Europe. *Molecular Ecology*, *7*, 453–464. https://doi.org/10.1046/j.1365-294x.1998.00289.x

Terrab, A., Schönswetter, P., Talavera, S., Vela, E., & Stuessy, T. F. (2008). Range-wide phylogeography of *Juniperus thurifera* L., a presumptive keystone species of western Mediterranean vegetation during cold stages of the Pleistocene. *Molecular Phylogenetics & Evolution*, *48*, 94–102. https://doi.org/10.1016/j.ympev.2008.03.018

Thiers, B. (2015). *Index Herbariorum: A global directory of public herbaria and associated staff*. New York: Botanical Garden's Virtual Herbarium. Retrieved from http://sweetgum.nybg.org/science/ih/

Thompson, J. D. (2005). *Plant evolution in the Mediterranean*. Oxford, UK: Oxford University Press. https://doi.org/10.1093/acprof:oso/9780198515340.001.0001

Thuiller, W. (2003). BIOMOD – optimizing predictions of species distributions and projecting potential future shifts under global change. *Global Change Biology*, *9*, 1353–1362. https://doi.org/10.1046/j.1365-2486.2003.00666.x

Tremetsberger, K., Ortiz, M. A., Terrab, A., Balao, F., Casimiro-Soriguer, R., Talavera, M., & Talavera, S. (2016). Phylogeography above the species level for perennial species in a composite genus. *AoB Plants*, *8*, 142–159. https://doi.org/10.1093/aobpla/plv142

Tripp, E. A., & McDade, L. A. (2014). A rich fossil record yields calibrated phylogeny for Acanthaceae (Lamiales) and evidence for marked biases in timing and directionality of intercontinental disjunctions. *Systematic Biology*, *63*, 660–684. https://doi.org/10.1093/sysbio/syu029

Urbani, M., Calvia, G., & Pisanu, S. (2013). *Carex panormitana* Guss. *Schede per una Lista Rossa della Flora vascolare e crittogamica Italiana*, *45*, 134–136.

Urbani, M., Gianguzzi, L., & Ilardi, V. (1995). Notes on the distribution and ecology of *Carex panormitana* Guss. (Cyperaceae). *Giornale Botanico Italiano*, *129*, 186.

Vargas, P. (2007). Are Macaronesian Islands refugia of relict plant lineages?: A molecular survey. In S. Weiss, & N. Ferrand (Eds.), *Phylogeography of Southern European Refugia*. Dordrecht: Springer.

Warren, D. L., Glor, R. E., & Turelly, M. (2008). Environmental niche equivalency versus conservatism: Quantitative approaches to niche evolution. *Evolution*, *62*, 2868–2883. https://doi.org/10.1111/j.1558-5646.2008.00482.x

Webb, C. O., Ackerly, D. D., McPeek, M. A., & Donoghue, M. J. (2002). Phylogenies and community ecology. *Annual Review of Ecology and Systematics*, *33*, 475–505. https://doi.org/10.1146/annurev.ecolsys.33.010802.150448

Wickham, H. (2009). *ggplot2: Elegant graphics for data analysis*. New York: Springer-Verlag. https://doi.org/10.1007/978-0-387-98141-3

Wiens, J. J. (2004a). Speciation and ecology revisited: Phylogenetic niche conservatism and the origin of species. *Evolution*, *58*, 193–197. https://doi.org/10.1111/j.0014-3820.2004.tb01586.x

Wiens, J. J. (2004b). What is speciation and how should we study it? *The American Naturalist*, *163*, 914–923. https://doi.org/10.1086/386552

Wiens, J. J., Ackerly, D. D., Allen, A. P., Anacker, B. L., Buckley, L. B., Cornell, H. V., … Hawkins, B. A. (2010). Niche conservatism as an emerging principle in ecology and conservation biology. *Ecology Letters*, *13*, 1310–1324. https://doi.org/10.1111/j.1461-0248.2010.01515.x

Wiens, J. J., & Graham, C. H. (2005). Niche conservatism: Integrating evolution, ecology, and conservation biology. *Annual Review of*

Ecology, Evolution, and Systematics, *36*, 519–539. https://doi.org/10.1146/annurev.ecolsys.36.102803.095431

Won, Y. J., & Hey, J. (2005). Divergence population genetics of chimpanzees. *Molecular Biology and Evolution*, *22*, 297–307.

Zitari, A., Tranchida-Lombardo, V., Cafasso, D., Noureddine, H., Scopece, G., & Cozzolino, S. (2011). The disjointed distribution of *Anacamptis longicornu* in the West-Mediterranean: The role of vicariance versus long-distance seed dispersal. *Taxon*, *60*, 1041–1049.

How to cite this article: Benítez-Benítez C, Escudero M, Rodríguez-Sánchez F, Martín-Bravo S, Jiménez-Mejías P. Pliocene–Pleistocene ecological niche evolution shapes the phylogeography of a Mediterranean plant group. *Mol Ecol*. 2018;27:1696–1713. https://doi.org/10.1111/mec.14567

SUPPORTING INFORMATION

Additional Supporting Information may be found online in the supporting information tab for this article.